JGR Atmospheres

RESEARCH ARTICLE
10.1029/2020JD034366

Arctic Cyclones and Their Interactions With the Declining Sea Ice: A Recent Climatology

E. Valkonen[1,2], J. Cassano[1,2], and E. Cassano[2]

[1]Department of Atmospheric and Oceanic Sciences, University of Colorado Boulder, Boulder, CO, USA, [2]National Snow and Ice Data Center, Cooperative Institute for Research in Environmental Sciences, University of Colorado Boulder, Boulder, CO, USA

Key Points:

- Less sea ice is related to higher cyclone track counts
- Less sea ice is related to stronger cyclones
- The new ERA5 reanalysis detects smaller cyclones than the ERA-Interim or CFSR data sets

Correspondence to:
E. Valkonen,
elina.valkonen@colorado.edu

Citation:
Valkonen, E., Cassano, J., & Cassano, E. (2021). Arctic cyclones and their interactions with the declining sea ice: A recent climatology. *Journal of Geophysical Research: Atmospheres*, *126*, e2020JD034366. https://doi.org/10.1029/2020JD034366

Received 7 DEC 2020
Accepted 30 MAY 2021

Abstract In this study, we applied a cyclone tracking algorithm to multiple reanalyses and categorized the detected cyclones based on season, intensity, and sea ice state to provide an Arctic cyclone climatology with emphasis on cyclone-sea ice interactions over the Arctic Ocean and adjacent waters. Our study period is from 1979 to 2015 and the reanalyses we are using are ERA-Interim, ERA5, and CFSR. As for our intensity variable, we use Accumulated Cyclone Energy (ACE), which has commonly been used as an intensity metric in the tropics but has not been utilized for high latitudes before. ACE has the advantage that it relates the cyclone intensity to the kinetic energy of the cyclone and therefore better represents the cyclone impact/interaction with the surface. We performed comparisons with the other more commonly used intensity metrics to assess the use of the ACE metric in the Arctic. Our main findings include increased cyclone counts with higher trends toward the end of the study period. Cold season cyclone counts were also found to be related to decreased sea ice concentration throughout the year. We also show that there is a relationship between the cyclone intensity measured by ACE and the surface state. Less sea ice was shown to be related to higher cyclone intensities. Comparisons between the the three reanalysis data sets are also presented.

Plain Language Summary In this study, three cyclone data sets were compared over the Arctic Ocean and adjacent waters to have a better understanding of how Arctic storms interact with the sea ice. Our study period is from 1979 to 2015, and we assessed multiple different storm characteristics, such as the size and intensity of the storm, to study the storms' relationships with the sea ice. We found that in the cold season (December–May), less sea ice was related to more and stronger cyclones, and that the amount of sea ice present had an influence on the cyclone strength over the study region.

1. Introduction

Middle and high latitude cyclones have an important role in everyday weather as well as in the Earth's climate system. Cyclones play an integral part in transporting energy, momentum, and moisture from the Equator to the Poles, in part enabling life on Earth (Bader et al., 2011; Ulbrich et al., 2009; Varino et al., 2018). In the polar regions, and more precisely in the Arctic, the unique environment in which the cyclones exist adds to the importance that cyclones play in the climate system (Simmonds & Keay, 2009; Zahn et al., 2018). A passing cyclone disturbs the sea ice field and can cause notable changes to both the sea ice surface and the ocean below (Graham et al., 2019; Simmonds & Keay, 2009). Graham et al. (2019) studied individual cyclones passing over sea ice during a field campaign over the Atlantic sector of the Arctic Ocean. They found that increased cloudiness related to the cyclone temporarily reduced ice growth due to decreased radiative cooling. Wind forcing from the cyclones would break the ice and enhance ocean-ice-atmosphere heat fluxes. They also discovered that increased snowpack associated with the storm hindered ice growth for the rest of the winter season, long after the cyclone had passed. These feedbacks are not readily observed in mid-latitudes, since only a few locations with sea ice exist and the temperature gradients between the ocean and atmosphere are usually smaller than in the Arctic.

Sea ice movement is largely determined by surface winds. Passing cyclones can cause sea ice buildup or open water areas by breaking the ice. They also carry with them large amounts of moisture and heat. This will prevent sea ice growth and support ice melt (Bader et al., 2011; Graham et al., 2019). A good example is the August 2012 storm discussed by Parkinson and Comiso (2013). The year 2012 had experienced lower

than normal Arctic sea ice extent, but the record-breaking low extent was due in part to a passing cyclone in August. The abnormally strong cyclone brought heat and moisture from the south into the Arctic. Strong winds broke off a large piece of the ice cover, and the exposed open water absorbed short wave radiation more efficiently, which led to increased surface warming. J. Zhang et al. (2013) modeled this "Great Arctic Cyclone" and found that increased vertical mixing in the oceanic boundary layer due to the strong winds associated with the storm also increased bottom melt of the ice. As shown by this case study, storms can have a strong impact on the sea ice (and oceanic boundary layer), especially in conditions where the sea ice has thinned and is thus more susceptible to movement by changes in wind forcing.

The effects of sea ice loss on the atmosphere can be divided into two categories: local and remote. Local effects include increased surface temperatures and upward heat and moisture fluxes, decreased static stability, and changes in cloud cover (Overland & Wang, 2010; Schweiger et al., 2008; Screen et al., 2013; Serreze et al., 2009). Remote effects include changes in atmospheric state (such as temperatures, sea level pressure [SLP], and precipitation) outside the immediate areas where the observed sea ice loss take place (Vihma, 2014).

Local effects were the focus of a study by Schweiger et al. (2008). They studied the cloud response to changes in SIC variability and found that decreases in SIC are related to increased cloud heights. They also determined that decreased SIC coincided with increased relative humidity near the surface, a deeper boundary layer, and more precipitation. This led them to conclude that an absence of sea ice decreased static stability in the boundary layer, reduced saturation near surface, but increased moisture higher up as moisture was transported further aloft due to stronger convection. This led to decreased low-level clouds but increased high-level clouds. Rinke et al. (2006) studied the atmospheric response to surface changes over the Arctic region using a regional climate model. They found that near-surface temperatures do respond to sea ice changes and this response has strong seasonality, with the strongest response in the winter season. It is evident from these studies that the strongest local response to sea ice decline is the warming of the surface. This response coincides with changes in moisture content, boundary layer stability, pressure patterns, etc. These studies demonstrate the strong local influences sea ice cover can have on the atmosphere. These changes can then also affect the atmospheric state more broadly in the following seasons and outside the Arctic.

Synoptic scale cyclones are mostly formed by baroclinic instability, which is affected by the horizontal temperature gradient and static stability. This formation can be strongly influenced by diabatic processes, depending on the type of the storm. Both baroclinicity and diabatic effects are affected by changing sea ice cover. It is therefore not surprising that changes in sea ice cover influence cyclones as well. Koyama et al. (2017) studied how summer sea ice loss influences cyclones in the following autumn and winter. They compared years with high versus low summer sea ice extent. They showed that over regions with strong sea ice loss in the summer, vertical stability decreased the following autumn/winter together with increased baroclinicity. These observed changes would favor cyclogenesis over the Arctic region. They also found that over sub-Arctic regions cyclones had become stronger in years with low summer sea ice extent. Similar results were found by Jaiser et al. (2012). They used ERA-Interim data to evaluate low and high sea ice years and how these affect both synoptic scale cyclones and planetary scale waves. They found that low ice years would favor earlier onset of baroclinicity poleward of 75°N. They also noted that the changes in baroclinicity would then influence planetary scale circulation and could contribute to a shift into the negative phase of the NAO. This is consistent with other studies on the topic (Alexander et al., 2004; Francis et al., 2009; Yamamoto et al., 2006). Simmonds and Keay (2009) evaluated September cyclones within the Arctic basin for 1979–2008. They compared high and low ice years with a focus on both cyclone numbers and a set of other cyclone properties. They discovered that decreased September sea ice is connected to increased mean cyclone size and depth in the same month. Cyclone frequency was not observed to change significantly.

In addition to studies relating sea ice changes to changes in cyclone frequencies, multiple studies have identified changes in cyclone frequencies and properties in a warming climate. X. Zhang et al. (2004) studied Arctic cyclones in relation to the changing climate. They applied an automated cyclone tracking scheme to reanalysis data for a time period of 1948–2002. They divided their study area into multiple sub-regions: Arctic Ocean, Arctic marginal zone, and the mid-latitudes. They found a lower number of cyclones in the Arctic Ocean than over sub-Arctic with strong seasonality, and a positive trend in the Arctic cyclone numbers

during the study period. McCabe et al. (2001) studied extratropical cyclones between 1959 and 1997 using reanalysis data and found increased cyclone counts in higher latitudes and decreased counts in the mid-latitudes. Wickström et al. (2019) aimed to strengthen the understanding of regional scale processes in the warming climate and used reanalysis data to conduct a composite analysis on cyclones around Svalbard. They found an increased number of cyclones near Svalbard with a warmer and wetter atmosphere for the winter season. A comprehensive review of Arctic sea ice changes, extratropical storms, and the NAO was provided by Bader et al. (2011). They evaluated both observational and modeling studies for the recent past and the future, and concluded that sea ice changes are likely to have an effect on the North Atlantic and Pacific storms. They concluded that even though there still are large uncertainties as to the cyclone responses to the warming Arctic and sea ice decline, less sea ice seems to lead to stronger storms and in mid-latitudes the storm tracks are forecasted to experience a poleward shift.

As discussed above, cyclones play an important role in the Arctic climate system. They both influence and are affected by the environment around them. And even though there has been a vast amount of research into extratropical cyclones, regional studies on Arctic cyclones have gained less attention—this is especially true for the central Arctic. The sea ice surface is a very prominent feature of the Arctic environment and is also a key component of the climate system, affecting atmospheric circulation, the radiative budget, and the hydrological cycle. An additional interest in the relationship between Arctic cyclones and sea ice is due to the observed strong Arctic amplification (Maslanik et al., 2007; Onarheim et al., 2018; Screen & Simmonds, 2010; J. Stroeve et al., 2008; J. C. Stroeve et al., 2012). The Arctic sea ice reached an observational minimum in September 2012, and there have been predictions for ice free summer conditions in the Arctic by 2050 (Onarheim et al., 2018). The feedbacks between decreasing sea ice cover and the atmosphere are an active area of research, and this study aims to contribute to this by providing a current Arctic cyclone climatology comparing three different reanalysis products and evaluating how cyclones vary as a function of sea ice state. As the Arctic is rapidly warming and sea ice is thinning, the interactions between sea ice and Arctic cyclones become even more important. This is the motivation behind the study presented here. The next section will discuss in detail the data and methods that were used. Section 3 follows with the cyclone climatology separated by the different cyclone characteristics. Section 4 will include a discussion and conclusions.

2. Data and Methods

2.1. Reanalyses

To better the understanding of advantages and issues with reanalyses over the Arctic region, we compared three global reanalyses in this study. ERA-Interim (ERA-I) from the European Centre for Medium Range Weather Forecasting (ECMWF) (Dee et al., 2011) was their most up-to-date reanalysis product at the start of this project. It has also been shown to be the most accurate reanalysis data set for multiple different variables (before the introduction of ERA5) (Lindsay et al., 2014; Tastula et al., 2013). ERA-I is compared with the equivalent product from the NCEP/NCAR suite, the Climate Forecasting System Reanalysis (CFSR) (Saha et al., 2010b, 2014), and the new reanalysis product from ECMWF, ERA5 (Hersbach et al., 2020), which was introduced in 2019. There have been studies showing that for certain surface variables CFSR is more accurate than ERA-I (E. Jakobson et al., 2012; Tastula et al., 2013). Since the interest in this study is on multiple surface variables, comparing the CFSR product to the two ECMWF products makes sense.

Both the ERA-I and CFSR products start in 1979 with ERA-I ending in August 2019 and CFSR continuing to the present date. Our focus will be from 1979 to 2015. Both reanalyses have 6-hourly time resolution though their spatial resolutions differ. The ERA-Interim native resolution is 79 km (T255 horizontal resolution) with 60 vertical levels. CFSR has a higher resolution of ~38 km (T382 horizontal resolution) and 64 vertical levels. The ERA5 product begins in 1950. Hourly output is available, but we will only use 6-hourly data from 1979 to 2015 consistent with the ERA-I and CFSR data sets. ERA5 has a spatial resolution of ~31 km (T639 horizontal resolution) with 137 vertical levels making it the highest resolution global reanalysis product to date. The variables we use are SLP, 10 m zonal and meridional winds, and sea ice concentration (SIC).

The three reanalyses use slightly different sea ice data/calculation methods. ERA-Interim and ERA5 are based on satellite data (a variety of satellite data products: NCEP-2D Var, NCEO OISST v2, NCEP RTG, OSTIA for ERA-I and HaddISST2, OSI SAF for ERA5), whereas CFSR uses combination of satellite products (such as GFSC Ice, NCEP operational analysis, AMSR-E) which are then assimilated to the sea ice model (Dee et al., 2011; Hersbach et al., 2020; Saha et al., 2010b, 2014).

All products have been regridded (as with all the other data we process) to a 50 km Equal-Area Scalable Earth v.1 (EASE) grid. The benefit of an equal-area map is that distortion of grid cells near the poles is negligible and the area of the grid cells is conserved globally.

2.2. Satellite Product

In addition to SIC from the reanalyses, data from a satellite composite of SIC was also used (Cavalieri et al., 1996). This was done to have an as consistent SIC record as possible. The satellite data that are used in this study is a product from the National Snow and Ice Data Center (NSIDC). The NSIDC uses the NASA Team algorithm from NASA Goddard to derive SIC from the surface brightness temperature data taking into account weather effects. The SIC product is a combination of different passive microwave sensors: Nimbus-7 Scanning Multichannel Microwave Radiometer (SMMR), the Defense Meteorological Satellite Program (DMSP) -F8, -F11, and -F13 Special Sensor Microwave/Imagers (SSM/Is), and the DMSP-F17 Special Sensor Microwave Imager/Sounder (SSMIS). The aim of this product was to provide an accurate, consistent time series that could be used for different climatological studies related to sea ice.

The SMMR brightness temperature product and the subsequent SIC was provided by the NASA Goddard Space Flight Center. The SIC (and brightness temperature used to calculate it) for the SSM/I and SSMIS instruments were done by NSIDC. There were multiple dates, especially early in the data set, for which data did not exist. For these dates, we looked for the next day's data. If the next day's data was available, then it was used instead. If this was not the case, for example, multiple consecutive days were missing, reanalysis data were used instead. Another case of missing data is caused by deficiencies in spatial coverage over the pole. Due to the orbits of the satellite, a circular area around the North Pole is missing. The size of the hole varies between the different instruments, the smallest with the SMMIS (0.029×10^6 km^2) and the largest with SMMR (1.19×10^6 km^2). We used a mask provided by the NSIDC to recognize the missing grid points, and for those grid cells we used reanalysis data instead.

2.3. Cyclone Tracking Algorithm

The cyclone tracks used in this study are acquired by applying a tracking algorithm to the SLP fields from the reanalysis data sets interpolated to a 50 km EASE grid. The algorithm, described by Crawford and Serreze (2016), builds upon an algorithm first developed by Serreze (1995). The tracking algorithm identifies a cyclone by comparing SLP at each grid point to the eight neighboring points. Elevations above 1500 m are masked out to prevent erroneous SLP values. When a minimum is found, it gets assigned an individual ID that then allows for tracking that specific cyclone while also identifying cyclone splits and merges. Each cyclone will also have a theoretical maximum propagation speed of 150 km/h that is based on values from previous research (such as Wernli & Schwierz, 2006). This theoretical maximum propagation speed is then used to calculate the maximum propagation distance for the actual tracking. In the next time step, cyclones are again identified based on the SLP minimum, and they are given individual IDs. Cyclone locations are then compared to cyclone locations from the previous time step. Cyclone locations that match (the cyclone lies within a circle that has a radius of the maximum distance) are connected to the cyclone centers from previous time steps by updating their ID to match the ID of the previous cyclone. Cyclones that do not have a match in the previous time step are considered new cyclones. Cyclone centers from previous time steps that do not have a corresponding center in the current time step are considered to have experienced lysis.

An advantage of using this tracking algorithm, compared to the other available ones, is that in addition to identifying the location of the cyclone the algorithm also identifies the cyclone area. Cyclone area is defined by the last closed isobar (2 hPa isobar interval is used) before another minimum or maximum is observed. If multi-center cyclones are allowed, multiple minimums are allowed to exist within the cyclone area. Most

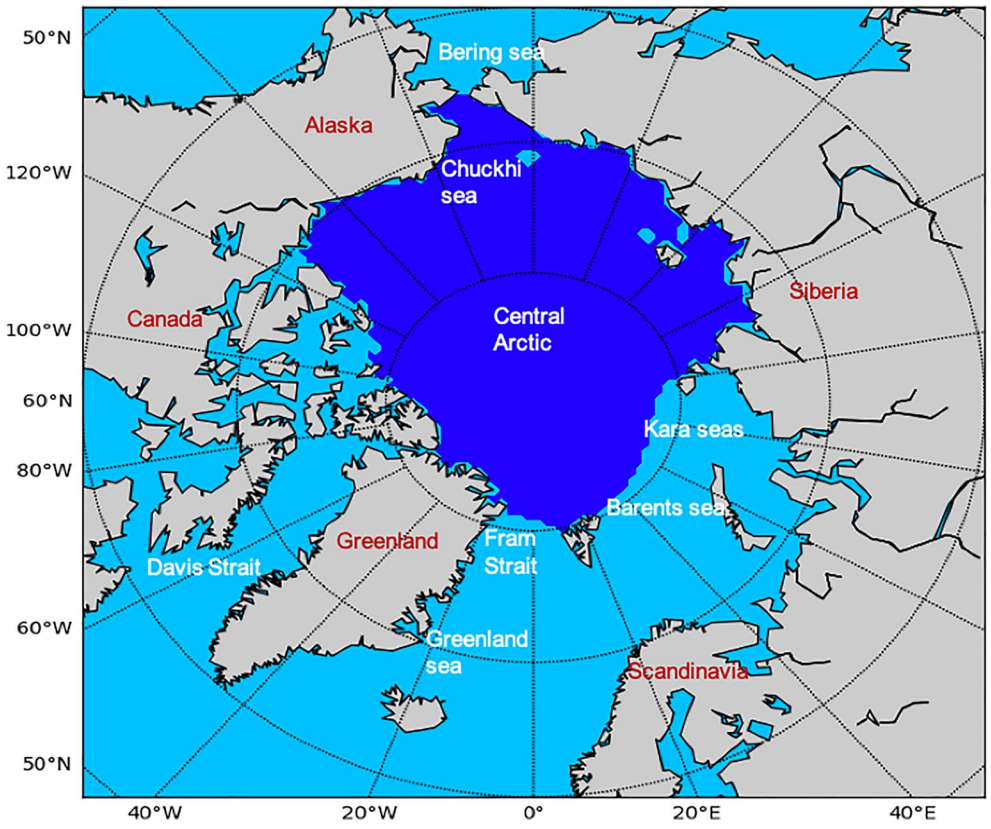

Figure 1. Map of the study region (blue) and outside the study region (light blue). Ocean locations are marked in white and locations over land are in dark red. Land areas are grayed out.

widely used algorithms do not provide cyclone area as part of their output. Some do consider area of the cyclone as they perform the tracking, but the area is not explicitly given in the output. Instead other metrics are given as a representation of the area/size of the cyclone, such as radius. An example of this kind of algorithm is the one by Murray and Simmonds (1991), which provides cyclone radius.

Even though there are criteria within the tracking algorithm to identify and disregard nonphysically weak systems, a few of these nonrealistic cyclones can still be found in the output from the algorithm. There were cases where a cyclone track existed, but the depth (central pressure minus edge pressure) of the system was zero. With all of these cases the area of the cyclone was one grid cell. These factors lead us to conclude that these zero-depth cases are not physically sound, and we have excluded these cyclone times from our analyses. If a zero-depth case took place in the middle of the cyclone track, the track was split into two separate tracks.

2.4. Cyclone Matrix

The focus of this study is on Arctic cyclones, but the tracking algorithm runs globally and provides only a subset of the variables we are interested in. Hence, some post-processing is needed. First, since our interest is on Arctic cyclones and their interactions with the sea ice, we only include cyclones that exist within our study region (the Central Arctic Ocean and adjacent Arctic Ocean waters, referred as "the Arctic" for the remainder of the paper (Figure 1) for at least 24 h. Restricting the study region to the Arctic Ocean will help keep the focus on the cyclone-sea ice-ocean interactions and the time requirement will help to reduce the number of weak, nonphysical depressions or cyclones that only briefly enter the study region. The time spent in the Arctic does not have to be continuous, the cyclones can move in and out of the Arctic during their lifetime, but the summed lifetime over the Arctic has to be at least 24 h for the cyclone to be included in the Arctic cyclone matrix.

The complexity of the Arctic climate system makes it difficult to try to find causal relationships between specific processes, because most of the time there are multiple factors contributing to the relationship. To try to untangle this complexity, we separate the cyclones into different categories. The categories used are season, sea ice state and intensity. This will help to focus on specific processes and provide more robust results.

The cyclone tracks are split into two seasons based on when they spend most of their time in the Arctic. Results are also shown for individual months in order to fully understand the seasonality in the cyclone climatology. The cold season is defined as December to May and the warm season June to November, approximately centered around sea ice maximum and minimum.

Sea ice state has three categories: open water, loose SIC ($15\% < \text{SIC} \geq 85\%$), and concentrated SIC (SIC >85%). We calculate SIC for each time step in two different ways. By calculating SIC at the central point of the cyclone, and by taking the mean SIC over the cyclone area.

There are many ways to define cyclone intensity. Our aim is to try to provide more insight into the relationship between Arctic cyclones and the sea ice and ocean surface. Therefore, we want to use an intensity metric that would provide as much information about the influence that the cyclone has on the surface. For the study presented here, we are introducing an intensity metric that has not been used in the Arctic before. It is called the Accumulated Cyclone Energy (ACE) metric. ACE is defined by Klotzbach (2006) as

$$\text{ACE} = (V_{max})^2$$

The ACE for this work is calculated in two ways:

$$\text{ACEmax} = (V_{area,max})^2$$

$$\text{ACEarea} = (V_{area-average})^2$$

ACEmax is the traditional metric described above, calculated with the maximum wind speed (V). The ACEarea is calculated to better capture the influence of the whole cyclone area instead of focusing only on the maximum wind speed. The intensity categories, based on percentiles of ACEarea for all Arctic cyclones for each season, are weak (<25th percentile), normal (25th–75th percentile), and strong (>75th percentile).

2.5. Analysis and Statistics

All cyclone properties discussed above, as well as other derived statistics, such as cyclone counts, are calculated for both cyclone tracks inside and outside of the Arctic, so Arctic cyclone characteristics can be contrasted with those outside of the Arctic. Similar to the requirement for Arctic cyclones tracks, all tracks outside of the Arctic are required to have a lifetime of 24 h or more. All time series calculations, as well as any spatial mean calculations are performed on seasonal means. Statistical significance is defined using a *t*-test for grid cells or time series that have 30 or more values. For grid cells or time series with less than 30 elements, a nonparametric significance test (Kolmogorov-Smirnov statistic on two samples) is performed. This is done to ensure that the assumptions behind the statistical significance testing are met. The biggest issue with our data with regard to statistical significance is that the data are highly skewed. Unless there are enough data points so that Central Limit Theorem can be applied, the assumption of normality would be broken. Nonparametric tests do not require predefined distributions, and hence are more accurate in cases with only a few data points. Statistical significance is reported at the 90% significance level in this study.

3. Results

3.1. Cyclone and Track Counts and Sizes

Figure 2 depicts the spatial distribution of cyclone counts for cold and warm seasons, and seasonal differences for the ERAI, ERA5, and CFSR reanalyses. The cold season shows an average of 2.0–2.5 cyclones per $(150\ \text{km})^2$ grid box in the Arctic (top row, Figure 2). These cyclones are mostly located on the North Atlantic side of the Arctic stretching from the Northern Barents and Kara Seas over to the Canadian Archipelago.

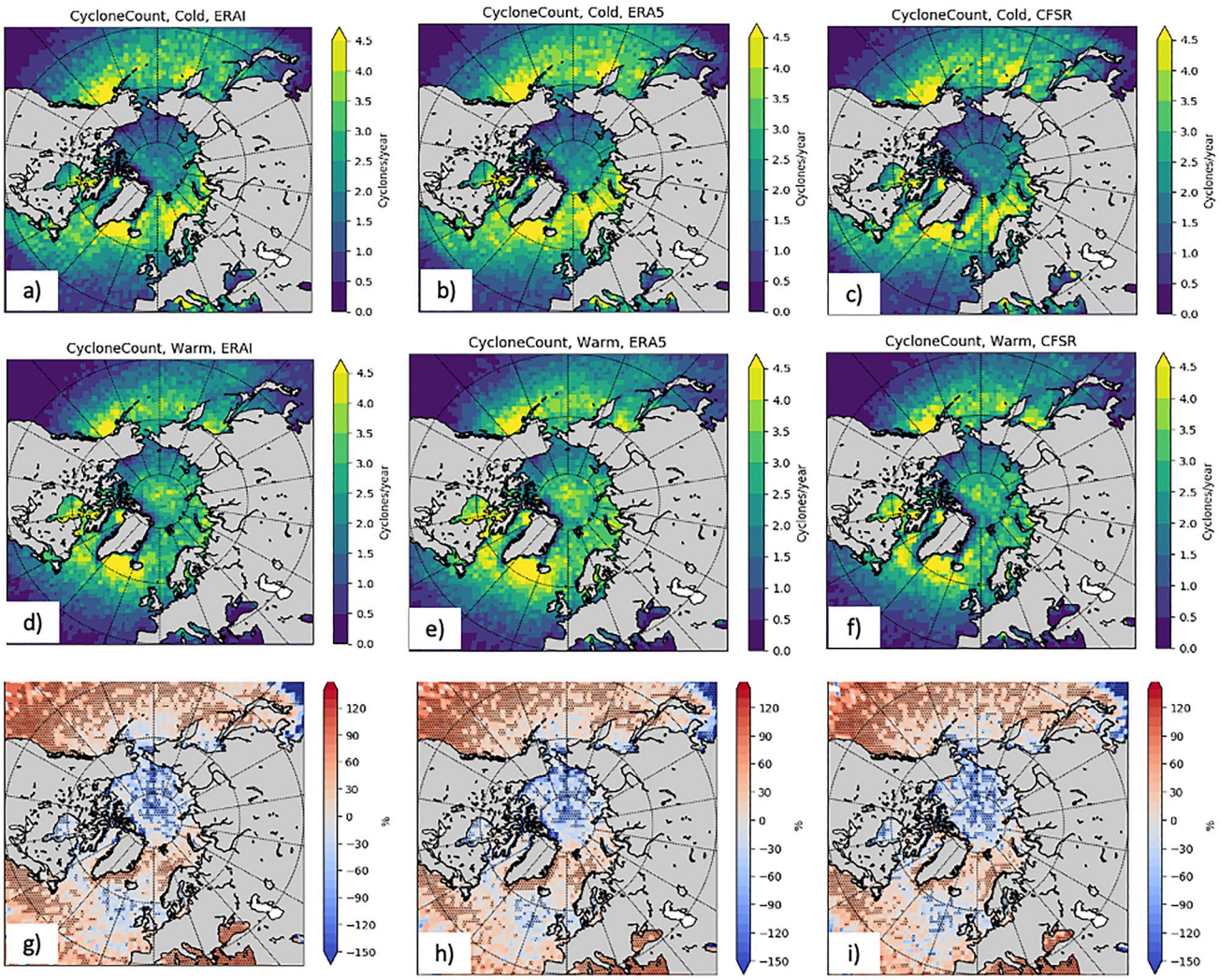

Figure 2. The seasonal average cyclone count for 1979–2015 calculated over 150 × 150 km grid boxes. Panels (a–c) show results for the cold season, and (d–f) for the warm season. The last row shows the difference between cold and the warm seasons. First column (a, d, and g) shows results for ERA-I data, the second column (b, e, and h) for ERA5 data, and the last column (c, f, and i) for CFSR. Statistically significant differences are shown by the stippling.

In the warm season, ~3.0–4.0 cyclone counts per (150 km)^2 grid box are observed in the Arctic, with most located in the Central Arctic (middle row, Figure 2). No statistically significant differences were found between the ERA-I, ERA5, and CFSR reanalyses (not shown).

The change in cyclone counts between the cold and warm seasons for ERA-I, ERA5, and CFSR are shown in the last row of Figure 2. The Central Arctic experiences around 60% less cyclones in the cold season compared to the warm season. The largest differences in seasonal cyclone counts are located in the central basin and Chukchi Sea areas with 60%–90% fewer cyclones in winter than in summer in these regions.

In addition to geographical variability, there is a strong seasonal variability in total cyclone tracks in the Arctic. Figure A1 shows the monthly distribution of total cyclone tracks in the Arctic for all three reanalyses. The highest counts are observed in September with lower values in the winter months. In the cold season, an average of 7–11 cyclones will pass through the Arctic in a month. In the warm season, this number increases to an average of 8–13 tracks in a month. The ERA5 reanalysis produces higher average monthly track counts followed by ERA-I and CFSR data sets. ERA-I shows generally slightly higher counts than CFSR.

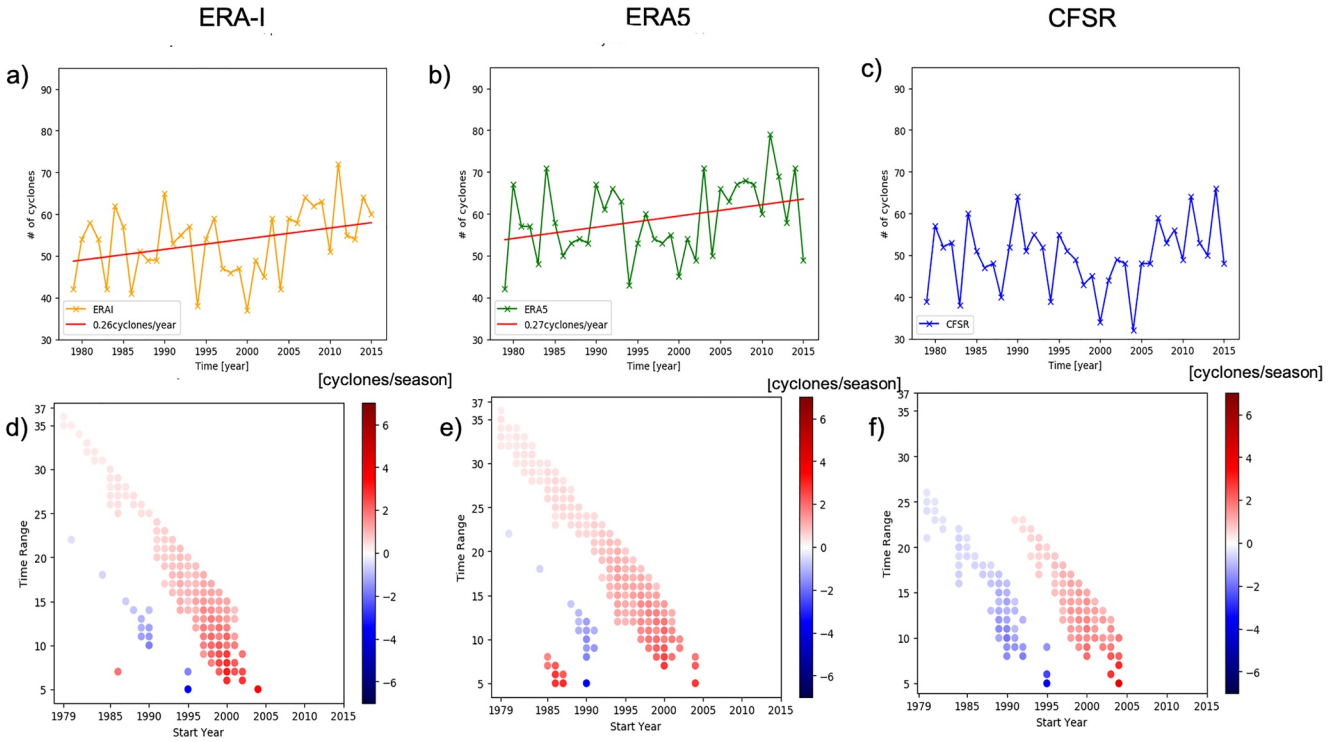

Figure 3. Timeseries and trends for yearly cyclone tracks in the Arctic (the study region) for 1979–2015. All the results are for the cold season. The first column shows ERA-I results, the middle ERA5, and right CFSR. The top row (a–c) shows annual cold season cyclone track counts in the Arctic, together with a line for statistically significant trends during the study period. The second row (d–f) shows statistically significant trends for different start years and time ranges. Panel (d) ERA-I, (e) ERA5, and (f) CFSR. Red (blue) colors mean positive (negative) trends.

Cyclone tracks also experience strong interannual variability in the Arctic as shown by the top row of Figure 3. In the cold season, the reanalysis data sets show between 31 and 79 cyclones in the Arctic per year, and the standard deviation of cyclone counts pers year ranges between 7.7 and 8.8 (CFSR and ERA5, respectively, with ERA-I at 8.3). The calculated trends show interesting features as well, shown in the bottom row of Figure 3. ERA-I and ERA5 experience mostly consistent positive trends throughout the study period, with strong increasingly positive trends starting in the 2000s and reaching as high as ~3.0 tracks/year. Shorter negative trends are observed in the early 1990s. The CFSR is mostly consistent with the two ECMWF products, but the early years of the study period do not show any significant trends and the positive trend pattern from the 2000s onward starts later. Time series and trend calculations were also performed for the warm season (Figure A2), but only short-term significant trends of between 5 and 15 years were observed.

The spatial distribution of cyclone radius is shown in Figure 4 (top and middle rows). The size of the cyclones exhibits spatial and seasonal variations. In the cold season in the Arctic, the largest cyclones are observed on the Barents and Kara Sea side of the Central Arctic, with an average radius of 1100–1300 km/cyclone. Smaller cyclones are found surrounding Greenland and north of Alaska, and they show an average radius of 500–700 km/cyclone. Interestingly, ERA5 represents the smallest cyclones, with statistically significant differences between ERA5 and ERAI/CFSR data products on the coast of the Arctic Ocean, surrounding Greenland and on the Pacific coast of Alaska and Asia (not shown). There were no statistically significant differences between the ERA-I and CFSR reanalyses. Seasonal differences in cyclone size (cold minus warm) were observed. The cyclones are generally smaller over the western Arctic Ocean in the cold season than in the warm season (Figure 4, last row), with around 10%–20% increase in size between the seasons compared to the cold season. No statistically different changes were found over the rest of the study area.

Figure 5 depicts the monthly distribution (a) and the interannual variability by seasons (b and c) of cyclone radius for cyclones existing in the Arctic for 24 h or more. In general, average cyclone size is the smallest

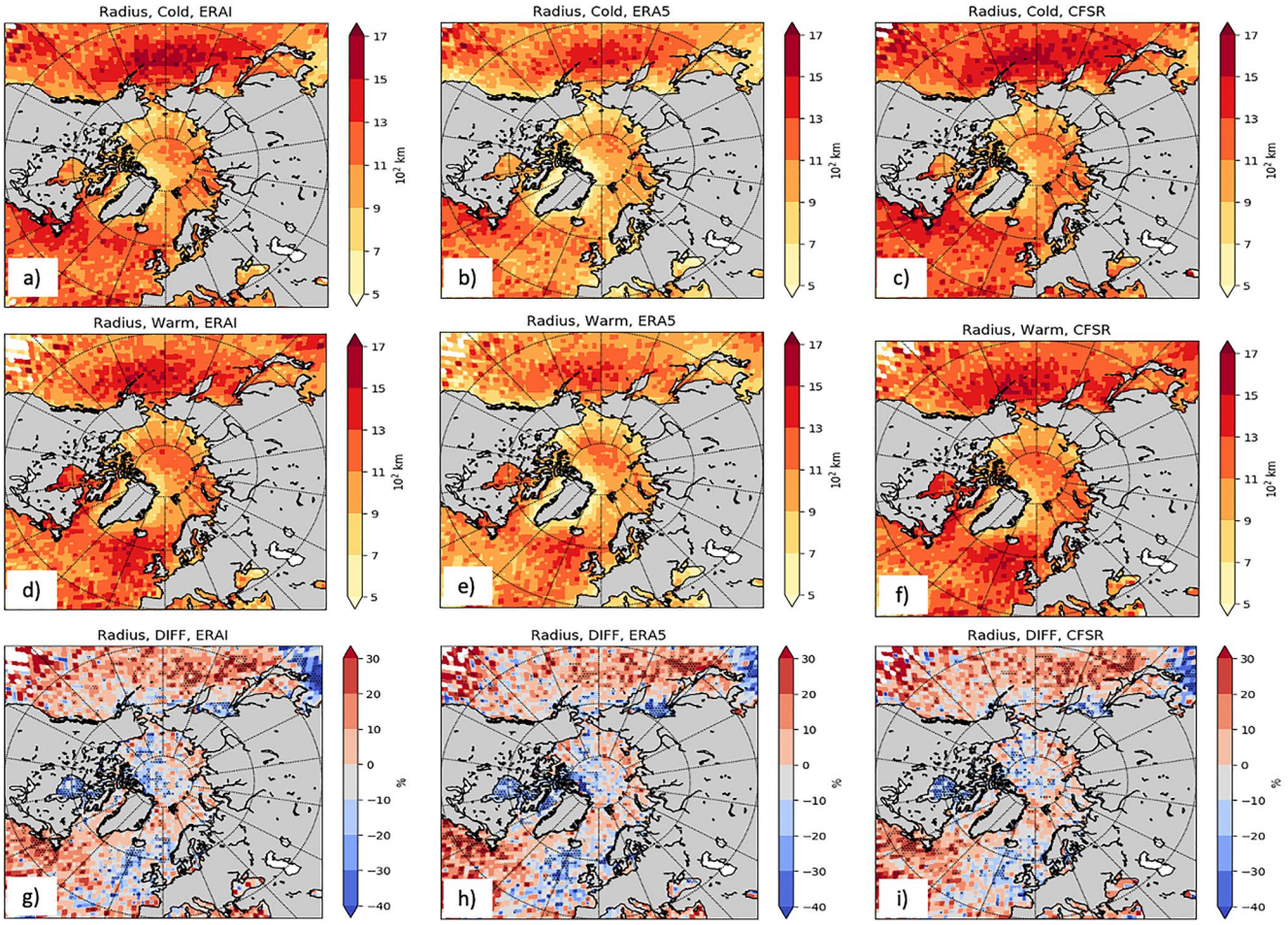

Figure 4. Average radius per cyclone at 150 × 150 km grid boxes. Results are shown for cold season (top row), and warm season (middle row). ERA-I data are shown in panels (a and d), ERA5 in panels (b and e), and CFSR in panels (c and f). The last row shows differences in average cyclone radius for 1979–2015 between cold and warm seasons (cold-warm). Results are calculated over 150 × 150 km grid boxes. Results are shown as a percentage change compared to cold season. The stippling shows the statistically significant differences at the 90% confidence level.

in the ERA5 product and largest in the CFSR data. Both monthly and yearly variability are observed. The largest median cyclone sizes within the Arctic are observed in the warm season, more precisely in July (1,100 km in July vs. 900 km in February/November) (a). The size of the cyclones reaches its maximum earlier in the year than the maximum number of cyclones (Figure A1). Strong interannual variability is also observed, together with a slight, but significant, negative trend in cyclone size (b and c, and Figure A3).

3.2. Cyclone Intensity

3.2.1. Spatial Variability

Figure 6 shows the spatial distribution of the multiple cyclone intensity metrics (the two ACE metrics, the average pressure gradient across the cyclone [DpDr], cyclone depth, central pressure [CentP], and the Laplacian of pressure [DsqP]) for the cold season. The corresponding figure for the warm season is found in Figure A4). The color bars are scaled such that areas with cyclones weaker than the median intensity are blue, and yellow to red colors show regions with intensities greater than the median.

In the cold season in the Arctic, the strongest cyclones are found on the North Atlantic side of the Arctic Basin. For ACEmax, ACEarea, central pressure, and depth metrics, the strongest cyclones stretch out toward the pole on the Siberian side of the basin, resembling the pattern for cyclone size spatial distribution shown in previous section. For the Laplacian of pressure and DpDr metrics, the pattern shows mostly even

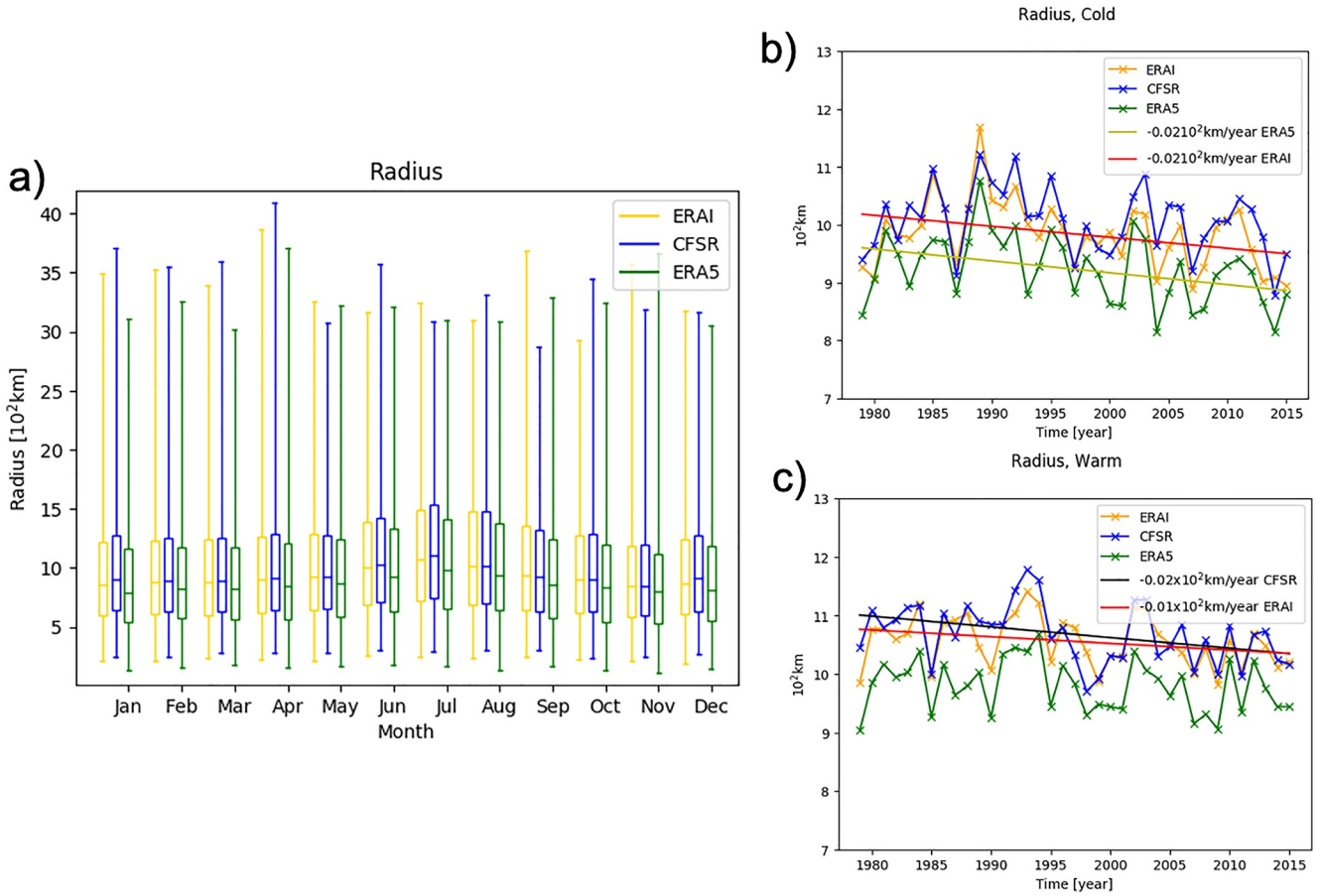

Figure 5. (a) Average monthly cyclone radius in the Arctic (within the study region) for 1979–2015. Boxes extend through the interquartile range, with median shown as a line and whiskers depicting minimum and maximum values. Time series of average seasonal cyclone radius for cold (b) and warm (c) seasons. The red line shows the statistically significant trend for ERA-I data, light green line for ERA5, and black for CFSR data. In all panels, yellow shows ERA-I data, dark green ERA5, and blue CFSR data.

distribution of cyclone intensities across the Central Arctic. For all the metrics, the weakest cyclones tend to be located north of Canada, stretching across/toward the Chukchi Sea along the northern Alaska coastline. Cyclones in the Arctic are weaker than their midlatitude counterparts over the North Atlantic and Pacific storm tracks. This holds true for all the intensity metrics for both seasons (Figures 6 and A4).

One important result seen in these figures is that spatially all of the metrics are consistent with each other. This includes the ACE metrics, which have not been previously used to characterize Arctic cyclones. The ACE metrics match the other metrics well spatially, depicting the midlatitude storm tracks and weaker cyclones over the Arctic Basin. This indicates that the broad patterns of cyclone intensity are consistent regardless of which intensity metric is used. It is also noteworthy that the relative cyclone strengths measured by the ACE metric are consistent with the other metrics. For example, in the cold season, cyclone intensities measured by central pressure, ACE or Laplacian over the study area are roughly between the 30th and 70th percentile range, while intensity measured by depth or DpDr is between the 40th and 70th percentile range. The seasonal variations are also evident in the ACE metrics, with relatively stronger cyclones in the Arctic in the warm season (top two rows, Figure A4) compared to cold season (top two rows, Figure 6).

Figure 7 shows the relative differences in intensities between ERA5 and CFSR (ERA5 minus CFSR) compared to the ERA5 for the cold season. Over the Arctic basin ERA5 produces consistently higher ACEmax and ACEarea values than CFSR. The relative differences between the two are around 20%–30% compared to ERA5 values. The area where ERA5 shows higher ACE values is larger in the cold season (panels a and b in Figure 7) than in the warm season (panels a and b in Figure A7) and appears to follow the sea ice edge.

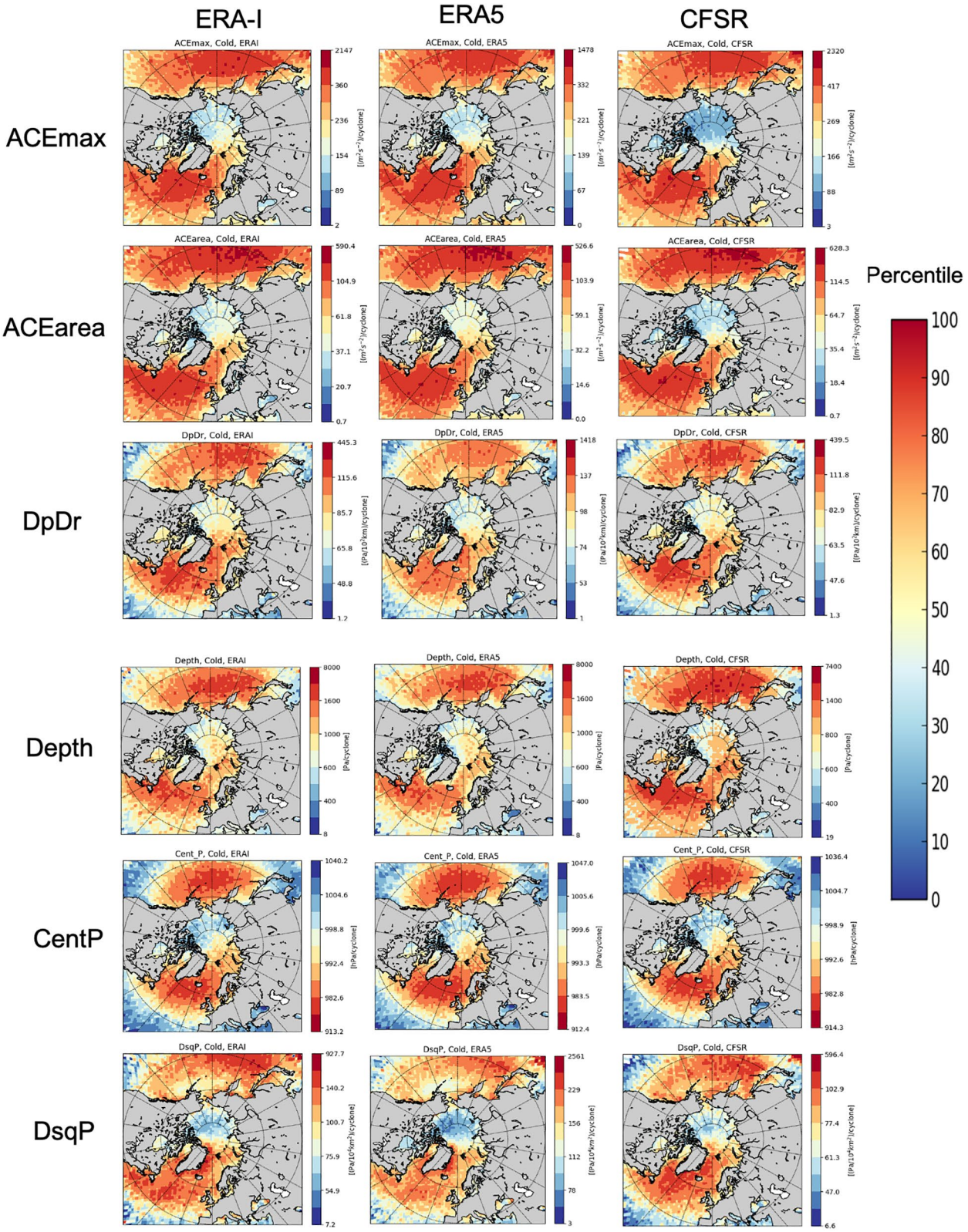

Figure 6. Different cyclone intensity metrics. The left column shows ERA-I data, middle column ERA5 data, and right column CFSR. Results are for the cold season. Intensity metrics were calculated as an average per cyclone in a 150 × 150 km grid box. The color maps were normalized based on the percentile values with red colors depicting stronger cyclones and blue colors weaker cyclones.

This is supported by the fact that ACE metrics display lower values in the sub-Arctic in ERA5 than CFSR; these differences are statistically significant over Northern North Atlantic, stretching from the East coast of United States to Scandinavia and over most of North Pacific. DpDr, depth, and central pressure show no significant differences between the two data sets inside the Arctic. The Laplacian of pressure has higher values in ERA5 than in CFSR, both inside the Arctic and over the mid-latitudes.

Results are very similar for comparisons between ERA-I and CFSR reanalyses in the cold season (Figure A5), whereas comparisons of the intensity metrics between the ERA5 and ERA-I in the Arctic show no statistically significant differences (Figure A6). The most pronounced difference between the two ECMWF products is the Laplacian of pressure, which is consistently lower overall in the ERA-I data set than in ERA5. Results for the warm season for all the data sets are consistent with the cold season results and can be found in Figures A7–A9.

Figure 8 shows the percent change in intensity metrics between the cold and warm (cold minus warm) seasons for CFSR, while Figure A10 shows this for the ERA5, and Figure A11 for ERA-I. In the Arctic, many of the metrics show weaker cyclones in the Chukchi sea/Canadian archipelago region in the cold season than in the warm season. The strength of this signal varies between the different metrics (DpDr, depth, and Laplacian all show a smaller area of weaker cyclones, and in most cases, these differences are not statistically significant). The most consistent signal is found for the central pressure intensity metric, which shows weaker cyclones in the cold season over most of the Arctic region. Weaker cold season cyclones are also found in the ACE metrics (more so in the CFSR data than with the ECMWF products). Based on all these different metrics, it is clear that over the Beaufort Sea, cyclones tend to be weaker in the cold season than in the warm season measured by the central pressure and energy they carry (the ACE metrics). As expected in the mid-latitudes, cyclones are stronger in the cold season than in the warm season in all reanalysis data sets.

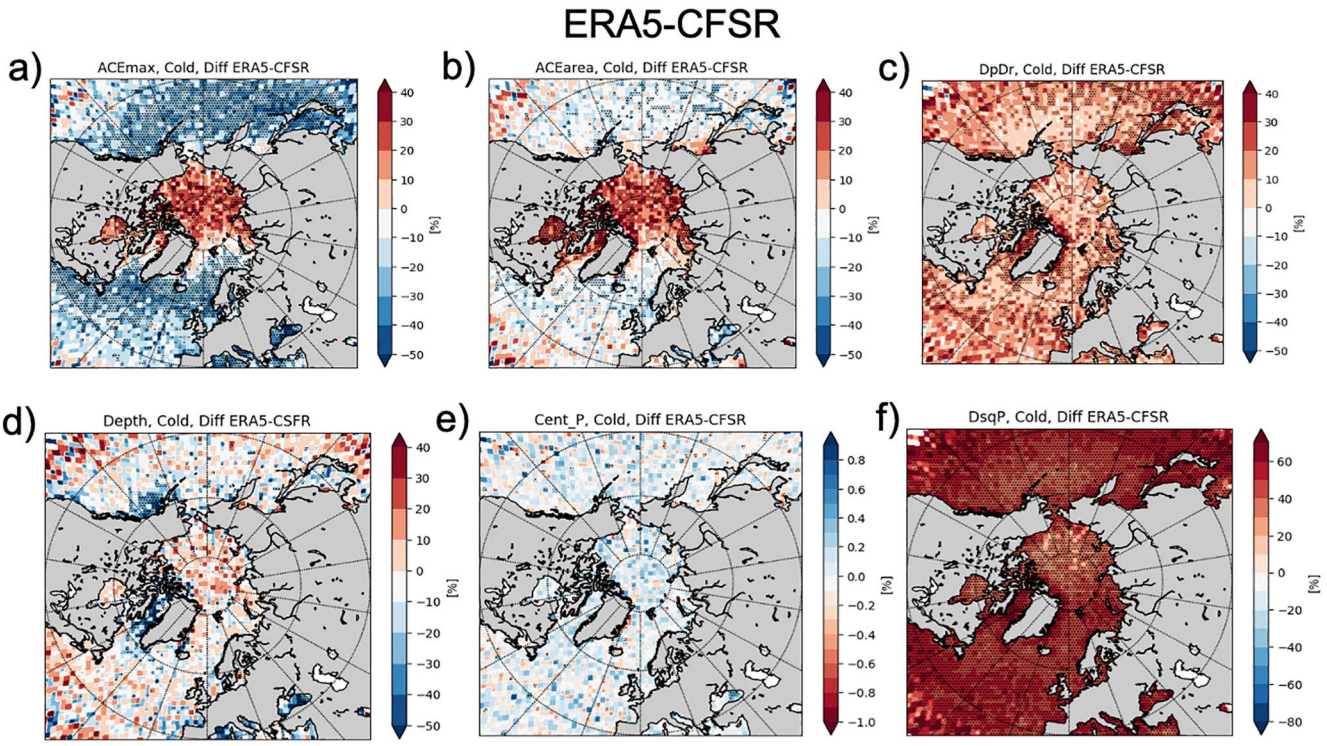

Figure 7. Differences in intensity metrics for the cold season (percentage change between ERA5 and CFSR compared to ERA5 data). Statistically significant areas, at 90% confidence level, are stippled. Red colors show positive change, blue colors negative change.

3.2.2. Frequency Distribution and Seasonal Variability

Figures 9 and A12 present the frequency distributions (first row) and their respective interannual variability (second row) for the different intensity metrics for the cold and warm season respectively. The frequency distributions for all metrics and all reanalyzes are similar (top row, Figure 9). The distributions are strongly skewed toward weaker intensity values (smaller ACE, DpDr, depth and Laplacian, and larger central pressure), with long tails for relatively infrequent strong cyclones.

The ERA5 and ERA-I reanalyses depict slightly higher intensity values than the CFSR for many of the intensity metrics. The frequency distributions of the ACE metrics and Laplacian of pressure in the cold season for the two ECMWF products tend to have more stronger cyclones than CFSR, whereas in the lower end of the distribution the CFSR reanalysis has higher counts (top row of panels a, b, and f in Figure 9). Depth, DpDr, and central pressure values are very similar between all of the reanalyses, consistent with the results shown in Figures 7, A5, and A6 for the cold season. Figure 9, bottom rows, depicts the interannual variability of the different intensity metrics. These are provided to help the readers to interpret the ACE trend matrices in Figures 10 and A13

Over the study period in the cold season, ERA5 and CFSR data showed a statistically significant negative trend in the ACEarea metric, whereas in the ACEmax metric, no statistically significant trend was observed in any of the reanalyses (bottom row in panels a) and b), Figure 9). However, in Figure 10, which shows the range of trends and their start years (similar to Figures 3, A2, and A3) for the ACEmax metric, we can see that both positive and negative trends of different lengths have existed over our analysis period. For the cold season, early in the study period, negative trends in intensity ranging between ~ -0.5 and $-6\frac{m^2}{s^2}$ /season were observed, but from the 1990s onward, intensities generally increased with an average trend of $\sim 4\frac{m^2}{s^2}$ / season (ERA-I) and $2\frac{m^2}{s^2}$ /season (ERA5/CFSR). In the warm season, the results are more mixed, depending on the reanalysis product used. Results for ACEarea are shown in Figure A13.

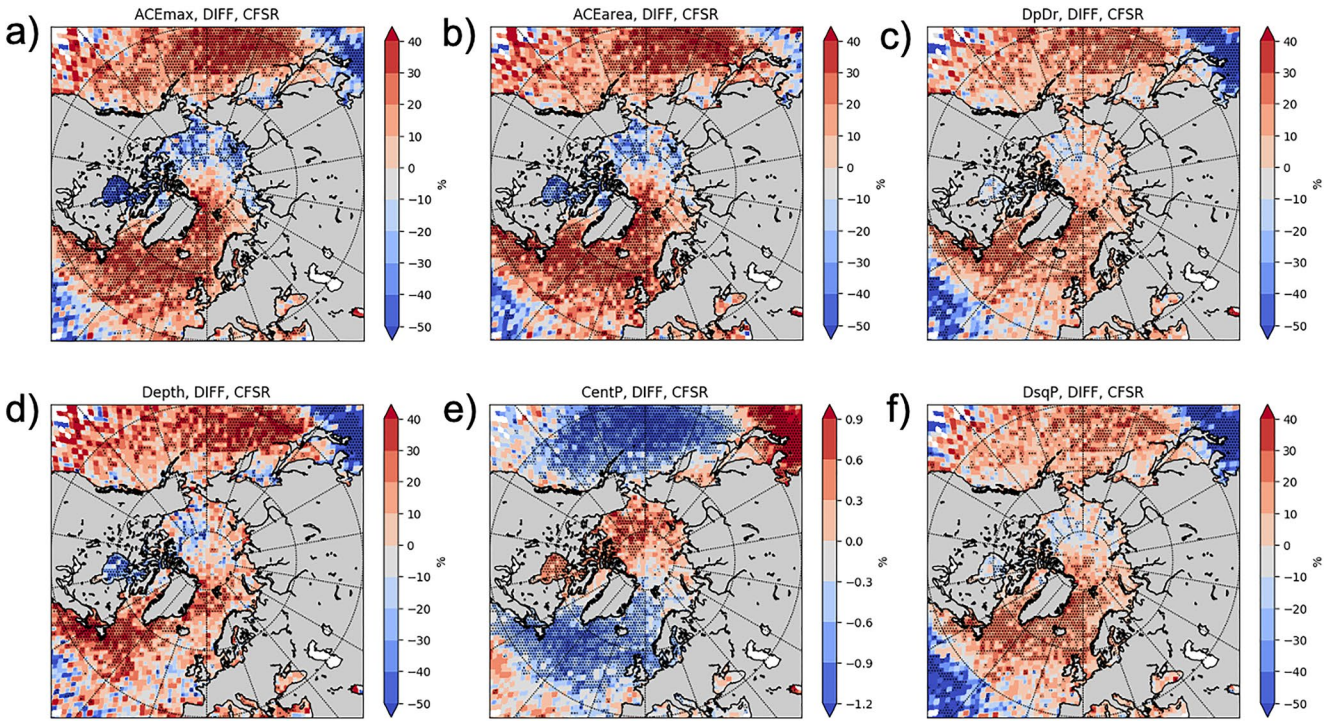

Figure 8. Difference in cyclone intensity between the seasons (percentage change between the cold and warm seasons compared to the cold season) for CFSR data. The difference is calculated as a percentage compared to cold season. Statistically significant areas, at 90% confidence level, are stippled. Red colors show positive difference and blue colors negative difference.

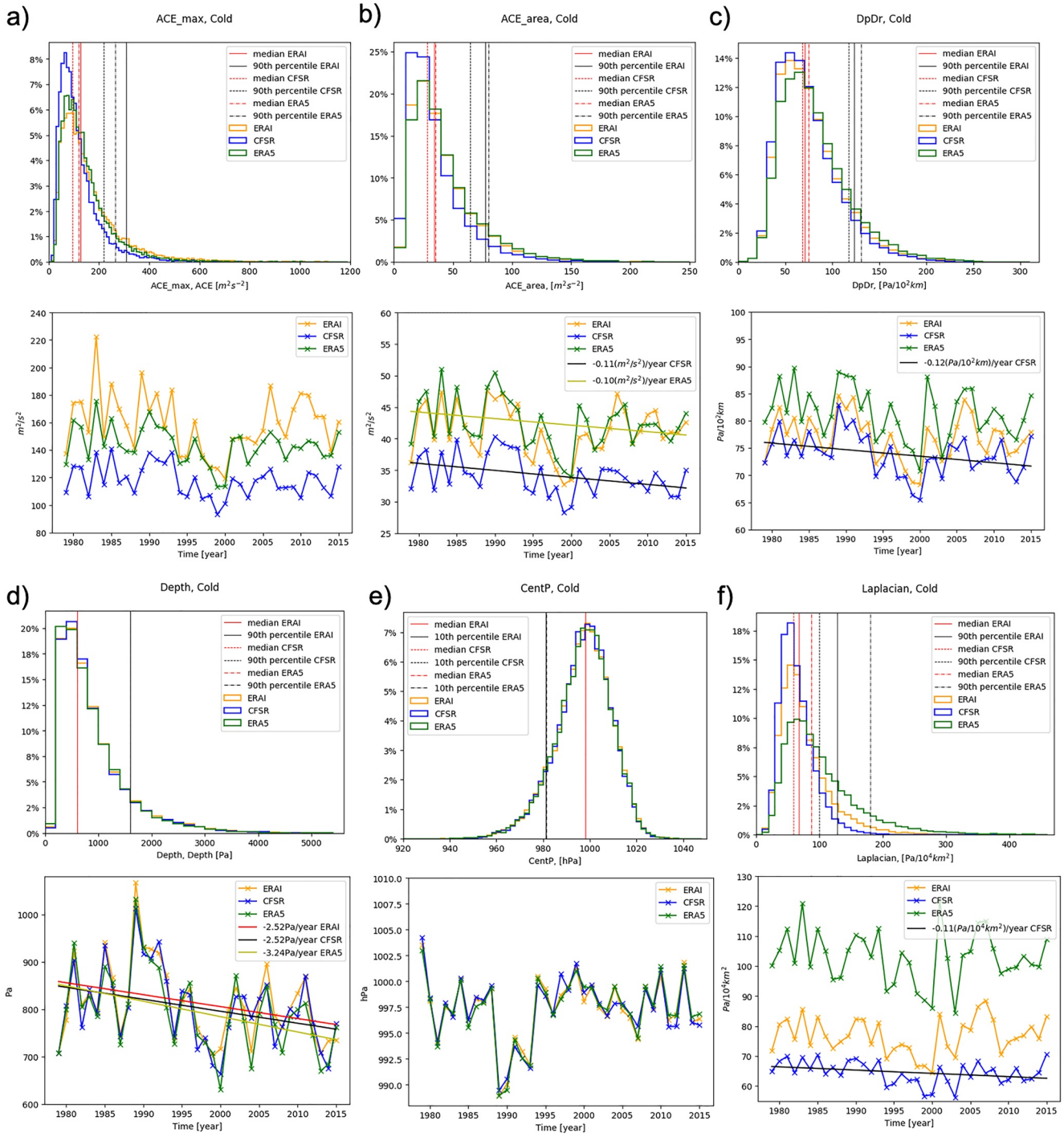

Figure 9. Cyclone intensity metrics for the cold season for the Arctic. The top row of each panel shows histograms created using data from individual cyclone timesteps for ERA-I (yellow bars and solid lines), ERA5 (green bars and solid lines), and CFSR (blue bars and dashed lines). Vertical red (black) lines show median (90th percentile) values. The second row displays seasonal time series of the corresponding intensity metric using the same color scheme as the top row for each reanalysis. Statistically significant trends at 90% confidence level are also shown (red lines for ERA-I, green for ERA5 data, and black for CFSR).

3.3. Sea Ice

Strong seasonal variability is clearly evident in Figure A14 which shows the monthly variability in cyclone area mean SIC for the ERA-I, ERA5, and CFSR reanalyses. The median SIC is shown to stay above 90% in the cold season with small interquartile ranges, whereas in the warm season, the median SIC is considerably

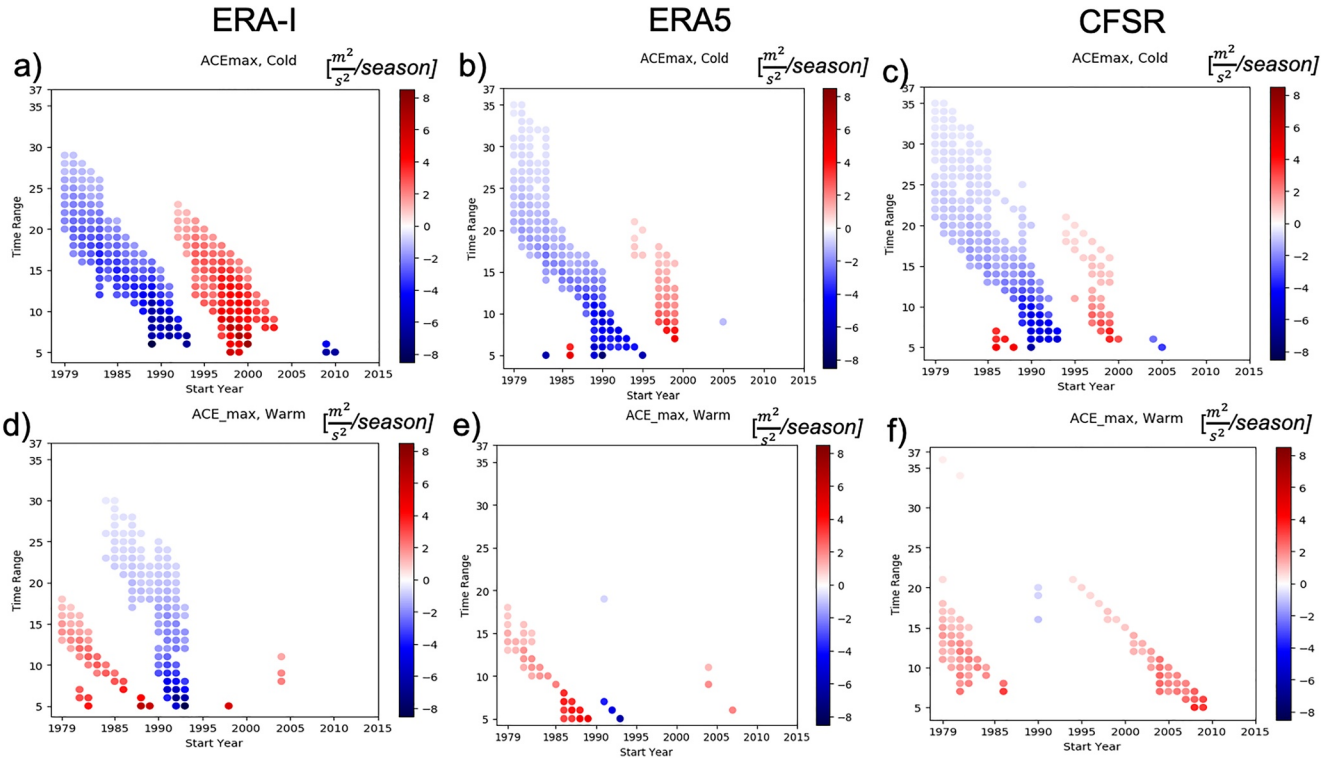

Figure 10. Trends for average ACEmax for different start years and time ranges for the Arctic. Red colors show positive trends and blue colors negative trends. All shown trends are statistically significant at 90% confidence level. Results are shown for cold (top row) and warm (bottom row) season for ERA-I (left column), ERA5 (middle column) and for CFSR (right column). Units are $(\frac{m^2}{s^2})$/year.

lower ranging between 70% and 90%, with distinctively larger interquartile ranges. SIC minimum is observed in September which also has the largest intra-monthly variability. Note that the SIC shown in these figures is the average SIC over the area of all cyclones in the study region and therefore does not represent the climatological SIC over the entire Arctic region that is regularly shown in the literature. Despite this difference, the results here do closely resemble the Arctic-wide mean, though are weighted by the areas that experience large cyclone counts and might underestimate areas with only few cyclones. Since the focus of this study is how cyclones interact with the sea ice, this variable is of essence to this study rather than a simple Arctic basin averaged SIC.

Figures 11 (warm season) and A15 (cold season) depict the basin wide seasonal distribution of SIC for 1979–2015, together with the significant trends over the study period. As with the monthly distributions interannual variability is also large in both seasons and all data sets. The standard deviation for the cold season is 1.18%/1.27%/1.32%, and for the warm season is 7.74%/8.19%/8.86% in ERA-I/ERA5/CFSR. In the cold season, the yearly mean varies between 98% and 91%, whereas in the warm season, the range is between 86% and 45%. Both seasons depict significant negative trends for the study period for all data sets. The strength of the trends depends on the time range and start year. For all data sets, the trend is stronger in the late 1990s and early 2000s. This is especially true for the warm season (Figures 11b–11d). This pattern resembles the trends for cold season cyclone counts (bottom row, Figure 3), but is opposite in the sign of the trend. Less sea ice in the late 90s and early 2000s seems to be associated with higher cyclone counts in the same time period.

3.3.1. Relationships Between Sea Ice and Cyclone Characteristics

Table 1 explores the relationships between cyclone track counts and sea ice displaying the Pearson correlation coefficient between the two for both seasons. The correlations were also calculated for detrended data and are shown in Table A1.The terms “Following” and “Preceding” are used with the sea ice seasons, when

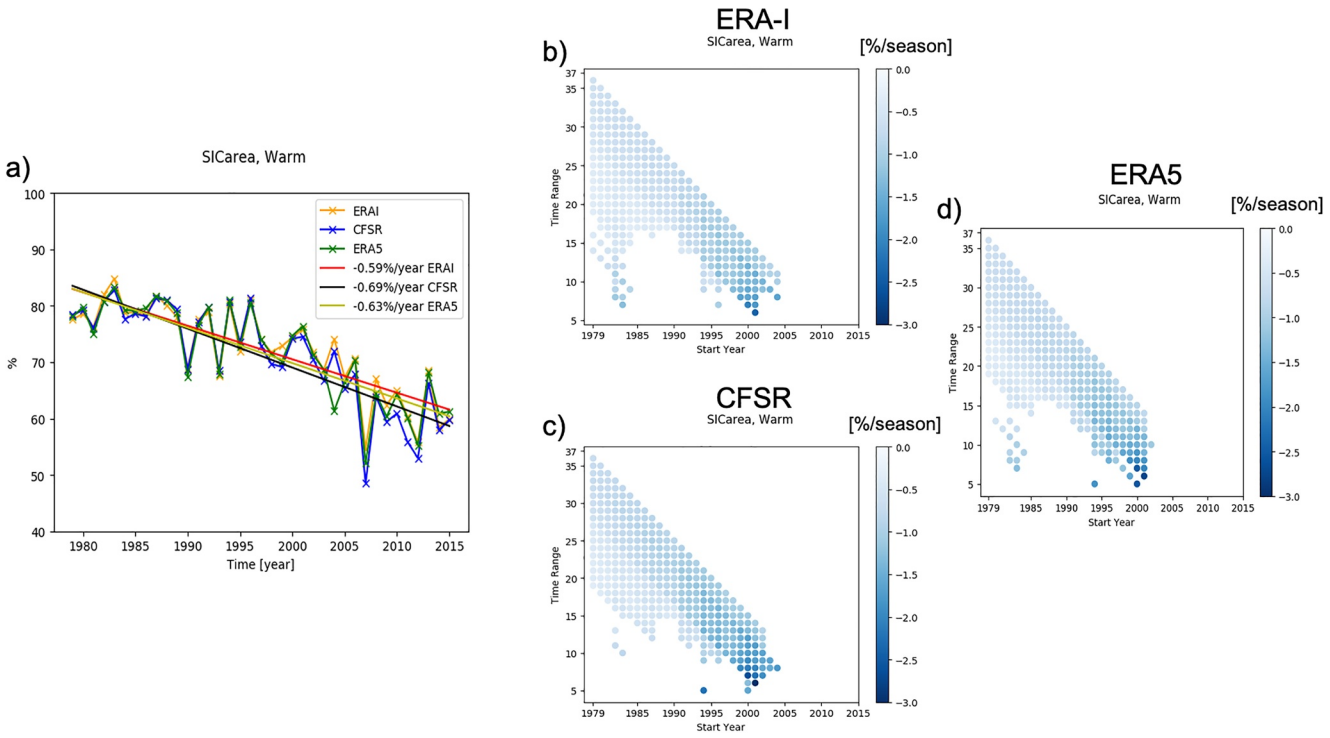

Figure 11. (a) Warm season time series of average SIC over the cyclone area for 1979–2015. Yellow color shows ERA-I data, green ERA5, and blue CFSR data. The red line shows the statistically significant trend for ERA-I data, green line for ERA5 and black data. (b) Trends for average SIC for a cyclone for different start years and time ranges for ERA-I data. (c) Similar to (b) but for CFSR data and (d) for ERA5 data. Results presented for the Arctic.

necessary, to depict, whether the sea ice season is the season after or before the season when the cyclones existed. There are no significant correlations between warm season cyclone tracks and sea ice. This is not surprising given that warm season track counts only showed variable and short (5–15 years) trends between 1995 and 2010 (Figure A2). However, cold season results show clear negative correlations between the cyclone tracks and SIC. All of the correlations between cold season cyclone counts and SIC for both seasons are negative and most of them are statistically significant, indicating that as SIC decreases, in both the warm and cold seasons, the number of cold season cyclones increases. Similar results were also observed between the detrended data sets (Table A1). The strongest correlation is found between cold season tracks and warm season SIC in the ERA-I data with a correlation of −0.55. The SIC does not appear to have an influence on the warm season cyclone tracks. This relationship between cold season cyclone tracks and sea ice was also suggested by the trend analysis before (Figures 3 and 11) with stronger positive cyclone trends in the cold season in the late 90s and early 2000s, and stronger negative trends in the SIC during the same time period. Similar trend patterns were also observed in the ACE metrics.

Table 1
Correlation Coefficients Between Cyclone Track Counts and Average SIC Over Cyclone Area for Different Seasons and for the Three Reanalysis Products

SIC	Cyclone tracks—COLD			SIC	Cyclone tracks—WARM		
	ERA-I	ERA5	CFSR		ERA-I	ERA5	CFSR
WARM (Preceding)	−0.24	−0.26	−0.03	COLD (Preceding)	0.03	−0.07	−0.08
COLD	**−0.45**	**−0.30**	−0.25	WARM	0.08	0.16	0.01
WARM (Following)	**−0.55**	**−0.47**	**−0.41**	COLD (Following)	−0.23	−0.03	−0.16

Note: Values that are statistically significant at 90% confidence level are in bold.

Table 2
Correlation Coefficients Between the ACE Metrics and Average SIC Over the Cyclone Area for Different Seasons and for the Three Reanalysis Products

SIC	ACEmax/ACEarea—COLD			SIC	ACEmax/ACEarea—WARM		
	ERA-I	ERA5	CFSR		ERA-I	ERA5	CFSR
WARM (Preceding)	0.05/0.06	0.25/**0.29**	0.22/**0.34**	COLD (Preceding)	0.02/0.00	−0.14/-0.14	−0.14/−0.08
COLD	−0.20/**−0.31**	**−0.41**/**−0.39**	**−0.34**/−0.26	WARM	0.15/0.19	0.06/0.10	**−0.32**/−0.08
WARM (Following)	−0.05/−0.05	0.12/0.12	0.17/0.26	COLD (Following)	**0.33**/0.21	0.04/0.04	−0.18/−0.04

Note: Values that are statistically significant at 90% confidence level are in bold.

How the average seasonal intensity of the cyclones, as measured by the ACE metrics, co-varies with the SIC was also evaluated. The results for both seasons are shown in Table 2 and for the detrended data in Table A2. Similarly, to track counts, less sea ice was associated with greater intensities, in the cold season. For ACEmax, ERA-I data showed a correlation of −0.20 (nonsignificant), ERA5 −0.41 (significant), and CFSR −0.34 (significant). Similar values were observed between ACEarea and SIC, −0.31 (significant) for ERA-I, −0.39 (significant) for ERA5, and −0.26 (nonsignificant) for CFSR. Consistent results were observed between the detrended data sets (Table A2). When the SIC was preceding the cold season cyclones, there were statistically significant positive correlations observed in few of the reanalysis data sets, but results were not consistent between the data sets and ACE metrics. CFSR data did also show statistically significant correlation between warm season tracks and warm season SIC (for the ACEmax, −0.32) and ERA-I for warm season cyclone tracks and following cold season SIC (0.33 for ACEmax). Based on the results presented here, the cyclone intensity measured by the ACE metrics is negatively correlated to the SIC, but this relationship seems to mostly exist in the cold season without seasonal lags.

The percentage distributions of cyclone intensity (based on ACEmax) for different sea ice states (open water, loose, and concentrated ice, defined in Section 2.4) are shown in Figure 12 for the cold and warm seasons. There are two main takeaways from this figure. First, through out the year, ERA-I and ERA5 data shows

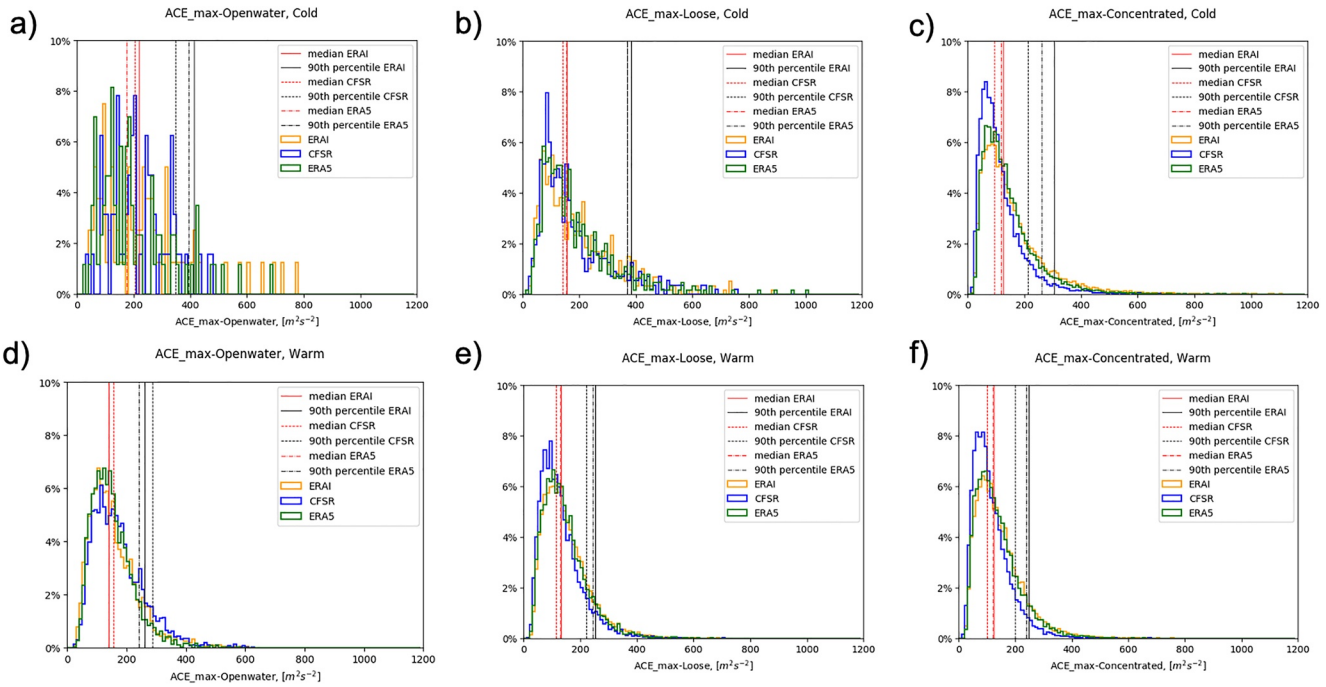

Figure 12. Histograms for ACEmax for cold and warm seasons separated by the different sea ice categories. The left column is open water, middle column is loose ice, and right column is concentrated ice. The top row is the cold season and the bottom row the warm season. Yellow bars show ERA-I data, green ERA5 and blue bars CFSR data. Median and 90th percentile values are represented by the red and black lines (solid for ERA-I, long dash for ERA5 and dashed for CFSR).

higher intensity values than CFSR for loose and concentrated ice categories. For example, in the cold season the median intensity for the loose ice category is $157\frac{m^2}{s^2}$ for ERA-I and $154\frac{m^2}{s^2}$ for ERA5, whereas it is clearly lower for CFSR with a value of $142\frac{m^2}{s^2}$. However, this difference between ERA-I/ERA5 and CFSR is not evenly distributed. CFSR shows higher frequencies of low intensity cyclones than ERA-I/ERA5, whereas the frequency of average to high intensity cyclones is higher in the ERA-I than CFSR. The open water category, however, shows contradicting results to the two sea ice categories for the warm season, with CFSR having higher median intensity than ERA5/ERA-I. For the cold season the number of open water cases is small so the results are less reliable. Second, cyclone intensity is observed to vary as the sea ice state changes. For the cold season, the median ACEmax (ERA-I/ERA5/CFSR) is $219\frac{m^2}{s^2}$ /$176\frac{m^2}{s^2}$ /$205\frac{m^2}{s^2}$ for the open water, around $157\frac{m^2}{s^2}$ /$154\frac{m^2}{s^2}$ /$142\frac{m^2}{s^2}$ for loose and a bit over $126\frac{m^2}{s^2}$ /$118\frac{m^2}{s^2}$ /$94\frac{m^2}{s^2}$ for the concentrated sea ice. Higher SIC values are associated with lower cyclone intensity distributions. This is consistent with findings in Tables 2 and A2.

Figures 13 (for strong cyclones) and A16 (for weak cyclones) show the percentage distributions for cyclone intensities for the different ice states for both seasons. The histograms are shown separately for the ERA-I, ERA5, and CFSR data sets, to highlight differences in cyclone intensity for the three different ice state conditions. Previous findings also suggest that stronger cyclones seem to interact with the surface more strongly than weak ones, which is why the results are shown separately for weak and strong cyclones. The definitions for strong and weak cyclones can be found in Section 2.4.

Figures 13 and A16 confirm the results shown by the previous histograms and Tables 2 and A2. As the SIC decreases, the (median) intensity of cyclones increases. In the cold season, cyclone (median) intensity (ERA-I/ERA5/CFSR) decreases as the surface category changes from open water ($366\frac{m^2}{s^2}$ /$335\frac{m^2}{s^2}$ /$302\frac{m^2}{s^2}$) to loose ($306\frac{m^2}{s^2}$ /$265\frac{m^2}{s^2}$ /$280\frac{m^2}{s^2}$) to concentrated ($275\frac{m^2}{s^2}$ /$239\frac{m^2}{s^2}$ /$207\frac{m^2}{s^2}$) for strong cyclones. This is also true for weak (Figure A16) cyclones, though the sensitivity of cyclone intensities to the sea ice state

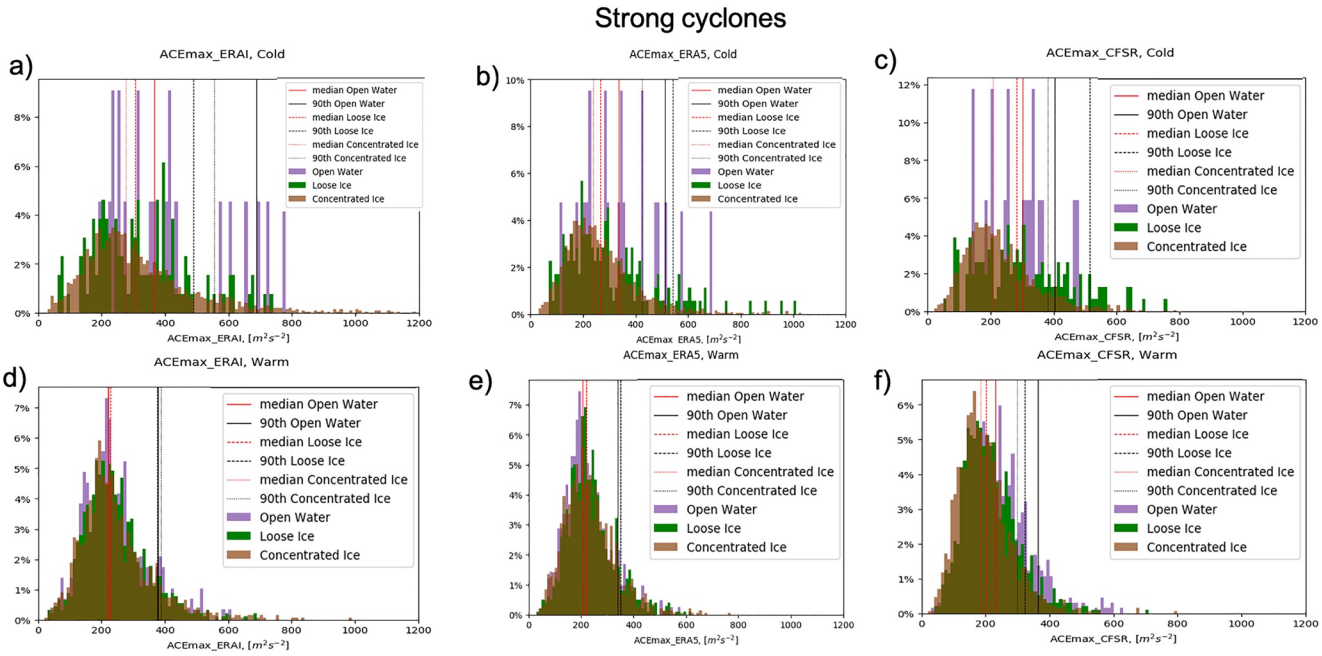

Figure 13. Histogram of ACEmax for different surface states for cold and warm seasons. Open Water is shown in purple bars, loose sea ice in green bars, and concentrated ice in brown bars. Only cyclones in the strong category are considered.

appears to be lower for the weak cyclones. However, there is a clear seasonal effect on this data, as warm season intensities are less sensitive to the sea ice category than cold season results. This is especially true for ERA-I data, which shows nearly identical results between the sea ice categories for warm season.

In general, the two ECMWF products are depicted to be less sensitive to the sea ice state than CFSR. In the cold season, the loose and concentrated sea ice categories have closer median values for ERA-I and ERA5, whereas the median intensity increases considerably with decreasing sea ice in CFSR. As mentioned above, this is even more apparent in the warm season, where the distributions of the different ice states are almost identical in the ERA-I data, but the intensity distribution shifts toward stronger cyclones with reduced sea ice in the CFSR reanalysis. Similar results are found for the weak cyclones. In most cases, lower SIC class is associated with higher intensities.

4. Conclusions and Discussion

The Arctic climate system is a complex system that has been changing rapidly, especially in recent years. As a consequence of the strong warming in the Arctic, sea ice has declined at an unprecedented pace. Cyclones play an important role in the interactions between the atmosphere and sea ice in the Arctic. Cyclones strongly impact the sea ice, but changes in the SICs can also affect the cyclones. This strong coupling between the sea ice and cyclones make it more difficult to assess the exact interactions between the cyclones and sea ice, especially in the context of the rapid changes taking place currently in the Arctic. To clarify these interactions, cyclones were divided into different categories based on three characteristics: season, intensity, and sea ice state. Here, cyclone characteristics were then compared between the three categories. A comprehensive climatology was produced with a focus on sea ice cyclone interactions.

The climatology presented in this study compares well with previous research. Seasonal track counts ranged from 31 to 72 cyclones in the Arctic in the cold season and 45 to 86 cyclones in the warm season (Figures 3 and A2). In the cold season, the cyclones were mostly located in the North Atlantic side stretching from Barents and Kara seas region to north of Greenland. In the warm season, the center of action is shifted toward the Chukchi Seas area, with maximum number of cyclones located in the Central Arctic (Figure 2). These spatial patterns match previous research well (Crawford & Serreze, 2016; Zahn et al., 2018; X. Zhang et al., 2004), as does seasonal variability (Figure A1). The observed warm season maximum in this study has also been demonstrated in many previous studies (Serreze et al., 2001; Serreze & Barrett, 2008; Zahn et al., 2018). Serreze and Barrett (2008) and, later, Crawford and Serreze (2016) attributed the observed summer maximum to higher cyclogenesis over the Siberian Plateau. Contradicting evidence has been provided by Simmonds et al. (2008), Sepp and Jaagus (2011), and more recently, Vessey et al. (2020). Simmonds et al. (2008) hypothesized that this difference could be due to a different tracking variable used by the different studies (mean sea level pressure (MSLP) versus relative vorticity/Laplacian of pressure). The median central pressure for cyclones in the Arctic was 998.1/998.2/998.1 hPa for the cold season and 995.4/995.5/995.5 hPa for the warm season (ERA-I/ERA5/CFSR) (Figures 9 and A12). In the warm season, the stronger cyclones also traversed further north, consistent with the seasonal cycle in cyclone numbers (Figures 6 and A4). The patterns for central pressure in X. Zhang et al. (2004) match the spatial distribution for central pressure in Figures 6 and A4.

In this study, a novel use for an intensity metric was demonstrated. The ACE metric has been previously used to analyze hurricane seasons in the tropics, but it was shown here that it is also a valid metric to use in the high latitudes. The ACE metrics are also shown to have a robust relationship with the sea ice (Table 2 and Figures 12, 13, and A16) depicting their value in providing insight into cyclone relationships with the surface. The results demonstrate that spatially the ACE metric is consistent with the other commonly used metrics. For example, in the cold season in the Arctic basin, cyclone intensities measured by ACE are between the 30th and 70th percentile ranges, compared with central pressure and the Laplacian of pressure which are also between the 30th and 70th percentile ranges, and with depth and DpDr which are between the 40th and 70th percentile ranges as shown by Figures 6 and A4. These together with the intensity probability distributions (Figures 9 and A12), which show similar shapes among all the intensity variables, show that the ACE metric can capture the important patterns in cyclone distributions and depict the seasonal cycle correctly. The good correspondence between the relative strengths measured by

the ACE metrics and the other more traditional metrics, together with the spatial distribution of the ACE metrics matching other metrics well, gives us confidence that the ACE metrics provide reasonable intensity values and are indeed valuable metrics to use to assess Arctic cyclones. In future work, we will focus mainly on the ACE intensity metrics since they are based on wind speed (kinetic energy) of the cyclone and thus give a more direct indication of how cyclones impact Arctic sea ice and the upper ocean through mechanical forcing.

An interesting feature is observed when the intensity metrics are compared between the ERA-I, ERA5, and CFSR reanalyses. Most of the metrics show no statistically significant difference between the three reanalyses in the Arctic, except for the ACE metric and the Laplacian of pressure (Figures 7 and A5–A9). In the Arctic, the ERA-I and ERA5 ACE metrics have higher values than in CFSR. This is quite unexpected as CFSR is the higher resolution reanalysis compared to ERA-I, and previous research (Vessey et al., 2020) has shown that higher resolution models tend to smooth wind fields less than lower resolution models, hence producing higher wind speeds. As such, one would expect CFSR to produce consistently higher ACE values than ERA-I, which is indeed true outside of the Arctic. The larger ERA-I/ERA5 values, compared to CFSR, appear to align well with the sea ice extent area (panels a and b in Figures 7, A5, A7, and A8). This suggests a systematic difference in how near-surface winds over sea ice surfaces are represented in ERA-I/ERA5 and CFSR. One of the more obvious explanations could be the surface roughness. The sea ice surface will, in general, have larger roughness than open water (e.g., Martin et al., 2014) and therefore, winds tend to be slower over sea ice than open water. CFSR has higher surface roughness over the sea ice than ERA-I/ERA5. This difference is roughly an order of magnitude, with CFSR surface roughness generally around 0.01 m with SIC higher than 10% and in ERA5/ERA-I ranging between 0.001 and 0.006 m depending on the SIC (ECMWF, 2006, 2016; L. Jakobson et al., 2019). This explains the difference in cyclone intensities (in ACE metrics) over the Arctic and also why this response is only taking place in the Arctic. This hypothesis is supported by the ACE histograms divided for different sea ice states (Figure 12). These figures depict that over sea ice surfaces ERA-I/ERA5 has higher intensity values than CFSR, whereas over open water, in the warm season, CFSR shows higher ACEmax values than ERA-I/ERA5.

Cyclone sizes between the different reanalyses were also compared (Figure 4). All the data sets showed smaller cyclones in the Arctic than over the mid-latitudes with a slight seasonal cycle. In the Arctic, specifically north of Greenland and the Canadian Archipelago, cyclones were smaller in the cold season than in the warm season. ERA-I and CFSR are very consistent with each other, whereas ERA5 shows smaller average cyclones (Figure 4) as well as smaller minimum cyclone sizes (Figure 5). This is not surprising as ERA5 has higher resolution than its two counterparts and will therefore be able to detect smaller cyclones. This appears to be the reason for the decrease in the average cyclone size, as more smaller cyclones are detected with ERA5 than ERA-I/CFSR reanalysis. Cyclones were also found to have become smaller (Figure 5) over time, though these trends do experience strong variability (Figure A3) depending on the season, start year and time range over which the trend has been calculated. In both seasons consistent long term (over periods from 5 to 36 years) negative trends around -0.1×10^2 km are observed until the early 1990s. ERA-I data in the cold season shows the most consistent negative trends. Increasing cyclone sizes are observed at the beginning of the study period in the cold season and for CFSR data also in the warm season. Similar to this study other studies looking into trends in cyclone sizes have found both negative (Zahn et al., 2018) and positive trends (Simmonds & Keay, 2009). This depicts the strong interannual variability in the size of the cyclones, which was also observed in this study (Figure 5).

One of the most intriguing results in our analysis of track counts was the strong positive trend in cyclone numbers from ~2,000 onward in the cold season (Figure 3) and its connection to the decreasing SIC. Increased number of cyclones has also been observed in many other studies (Rudeva & Simmonds, 2015; Sepp & Jaagus, 2011; Zahn et al., 2018), but the positive trends found in Sepp and Jaagus (2011) and Zahn et al. (2018) were not spatially coherent, and some studies have also found negative or nonsignificant cyclone trends (e.g., Simmonds & Keay, 2009). The connection between cyclones and the changing sea ice surface has also remained unclear. The results presented here show a more coherent cold season increase in the cyclone counts than previous studies have. We also showed that the increased cyclone

counts in the cold season were indeed connected to the declining sea ice in both the warm and cold seasons (Figures 11and A15). Less sea ice in the cold season or the following warm season was related to increased cyclone counts in the cold season. This was apparent in both the correlation tables and trend matrix figures (Tables 1 and A1, and Figures 3, 11, and A15). The negative correlation between the warm season SIC and cold season cyclones could be supported by the findings of Koyama et al. (2017), which connected low summer sea ice years with more favored conditions for cyclogenesis the following fall/winter. However, they did not find an increase in the number of cyclones associated with the declining sea ice, which our results clearly showed. The robustness of our results could be due to the use of more modern reanalysis data sets and/or the more targeted methodology used in this study compared to the analysis by Koyama et al. (2017), such as the focus on the Arctic Ocean area and cyclones that exist in the Arctic for 24 h or more.

Another explanation for less sea ice being associated with more cyclones could be through cyclones affecting the sea ice. The correlation between cyclones and SIC was observed to be stronger when the cold season cyclones preceded the SIC, implying a causal connection with cyclones causing changes in the the sea ice. This could be due to the cyclones reducing ice growth in the cold season and hence causing stronger ice melt in the warm season. More cyclones could also break more ice and transport it out of the immediate cyclone area, thus decreasing the SIC. This interaction could be enhanced by the thinning of the sea ice, which would be why the strong negative trend in sea ice is associated with the strong positive trend in cyclone numbers from 2000s onward. Sepp and Jaagus (2011) along with many other studies have shown that the number of cyclones entering the Arctic has increased (poleward movement of the North Atlantic storm track), supporting this theory. It is not, however, possible to determine which of these hypotheses would be correct with the current analysis presented here. Given the strong coupling of the ocean and atmosphere in the Arctic, most likely the result is a combination of both hypotheses, but the possibility of an unknown process affecting both variables cannot be excluded either.

Another interesting finding is the relationship between sea ice and cyclone intensity (measured by the ACE metrics). Less sea ice was shown to be associated with stronger cyclones in the cold season (Tables 2 and A2). The strongest sea ice decline (Figures 11 and A15) has been seen over the last 20 years, coinciding with the time range when the cyclone intensity trend matrices (Figure 10) and show increasing intensities for the cyclones. This is consistent with the correlation results in Tables 2 and A2 providing more robust results than the trend matrices or correlation results alone. The observed increased intensity with less sea ice was also discovered by Simmonds and Keay (2009) who showed that decreased September SIC was related to increased cyclone depth. Koyama et al. (2017) also found cyclones (in certain parts) in the Arctic to be stronger following years with low SIC, which they associated with increased baroclinicity. Our study also found that over open water cyclones tend to be stronger than over sea ice surfaces (Figures 12, 13, and A16) through comparing the cyclone intensity distributions with regards to different surface properties provide additional robustness to the relationship between sea ice and cyclones. In addition to changing baroclinity and increased moisture contributing to the intensity of the cyclones, the roughness of the open water/sea ice surfaces can also play a role, supported by the fact that the surface roughness appeared to influence the ACE metrics compared between the three different reanalyses (panels a and b in Figures 7, A6, and A7).

Tables 1 and A1 did imply causality between the SIC and cyclone counts, but the causality in relationship between SIC and cyclone intensity (Figures 13 and A16 and Tables 2 and A2) remains less clear. The coherently statistically significant correlation between the two is not lagged, as was the case between cyclone counts and SIC, and could be coincidental with stronger cyclones happening to be located where more sea ice is also located. Ignoring the possibility of coincidence, the question still remains as to what degree this increase in intensity is related to surface roughness, increased fluxes from the ocean, or to some other processes that are still unaccounted for.

Our work has highlighted the important role cyclones play in the Arctic system and their intertwined relationships with the sea ice surface in a more robust manner than previous research. We have shown that there is a relationship between Arctic cyclones and the sea ice surface, but the causality of this relationship still remains an open question and will be the focus of future work.

Appendix A: Additional Tables and Figures

Table A1
Correlation Coefficients Between Detrended Cyclone Track Counts and Detrended Average SIC Over Cyclone Area for Different Seasons and for the Three Reanalysis Products

SIC	Cyclone tracks—COLD			SIC	Cyclone tracks—WARM		
	ERA-I	ERA5	CFSR		ERA-I	ERA5	CFSR
WARM (Preceding)	−0.01	−0.09	0.06	COLD (Preceding)	−0.26	−0.03	−0.13
COLD	**−0.38**	**−0.32**	−0.22	WARM	0.23	0.25	0.18
WARM (Following)	**−0.52**	**−0.37**	**−0.53**	COLD (Following)	−0.01	−0.07	−0.04

Note: Values that are statistically significant at 90% confidence level are in bold.

Table A2
Correlation Coefficients Between Detrended ACE Metrics and Detrended Average SIC Over the Cyclone Area for Different Seasons and for the Three Reanalysis Products. Values That Are Statistically Significant at 90% Confidence Level Are in Bold

SIC	ACEmax/ACEarea—COLD			SIC	ACEmax/ACEarea—WARM		
	ERA-I	ERA5	CFSR		ERA-I	ERA5	CFSR
WARM (Preceding)	−0.22/−0.15	0.02/0.03	−0.1/−0.05	COLD (Preceding)	**0.3**/0.18	0.04/0.04	−0.11/−0.02
COLD	**−0.30**/**−0.42**	**−0.42**/**−0.40**	**−0.46**/**−0.42**	WARM	0.13/0.19	**0.31**/0.27	−0.12/0.04
WARM (Following)	−0.14/−0.25	−0.17/−0.20	−0.12/−0.13	COLD (Following	−0.02/−0.03	−0.04/−0.14	−0.14/−0.03

Note: Values that are statistically significant at 90% confidence level are in bold.

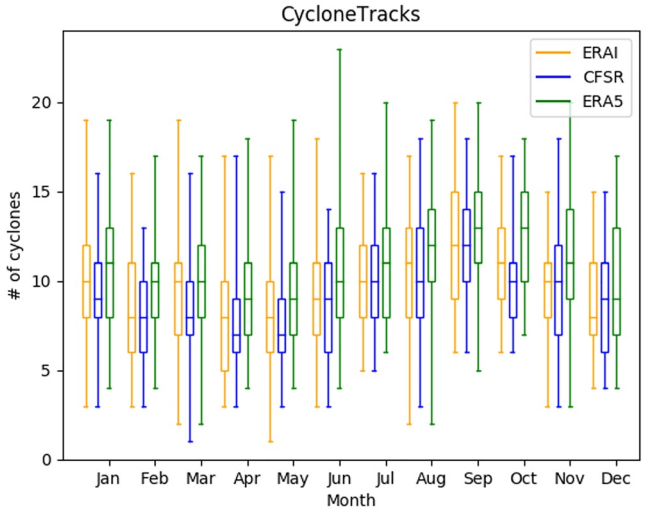

Figure A1. Average monthly cyclone tracks in the Arctic (within the study region) for 1979–2015. Boxes extend through the interquartile range, with median shown as a line, and whiskers depicting maximum and minimum values. Yellow boxes show data for ERA-I, green ERA5, and blue for CFSR.

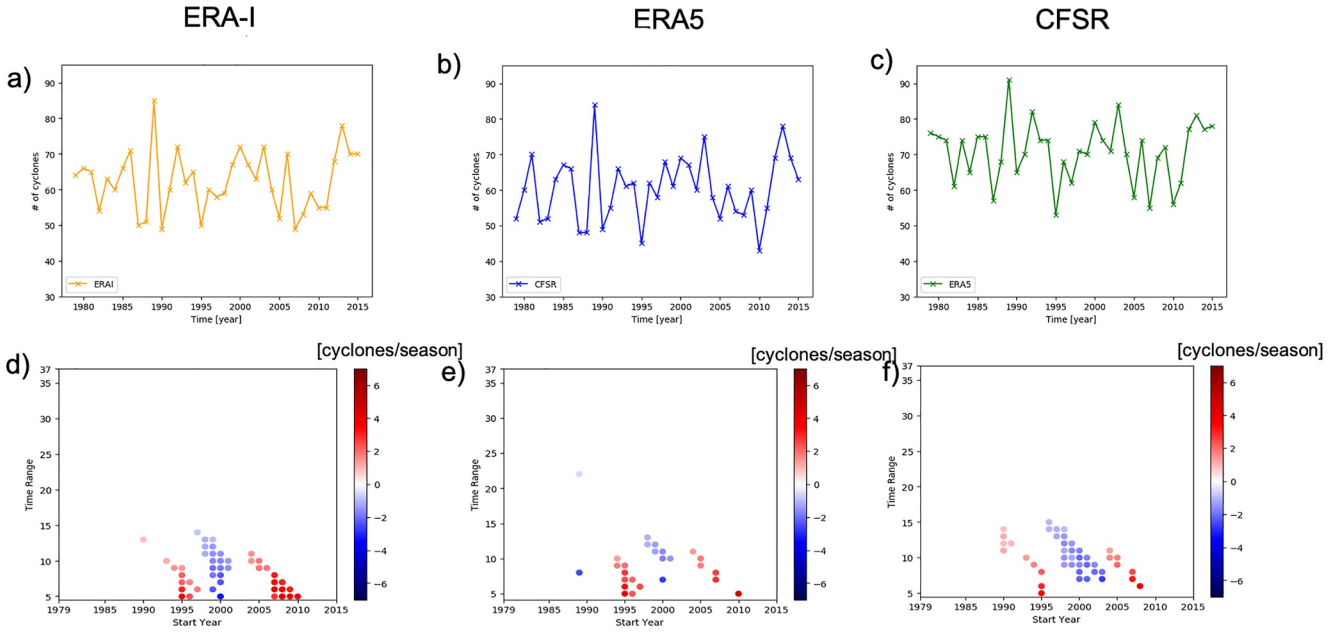

Figure A2. Time series and trends for warm season cyclone tracks in the Arctic for 1979–2015. First column shows ERA-I results, the middle ERA5, and the right CFSR. The top row (a–c) shows annual warm season cyclone track count in the Arctic. The second row shows (d–f) statistically significant trends for different start years and time ranges. Red (blue) colors are positive (negative trends).

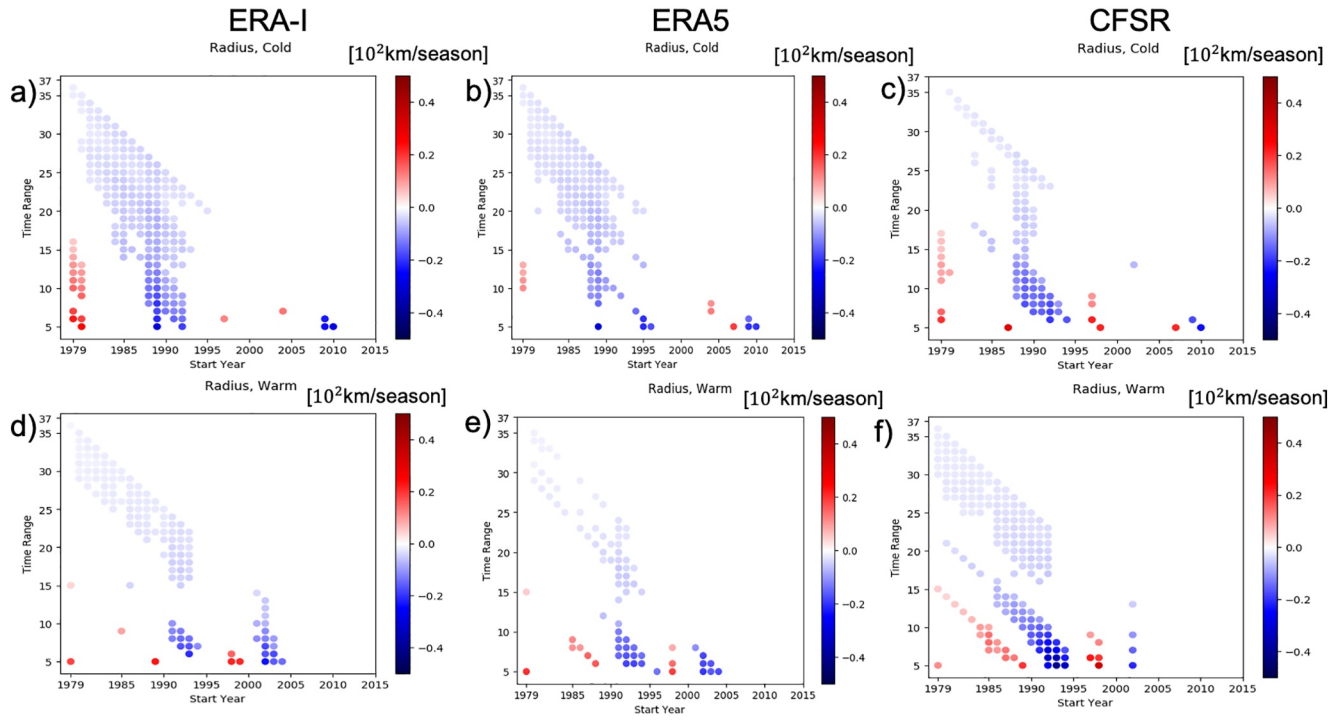

Figure A3. Trends for average cyclone radius for different start years and time ranges. Results are shown for cold (top row) and warm (bottom row) season and first column shows ERA-I data, second ERA5, and last column CFSR. Red colors show positive trends, blue colors negative trends. All shown trends are statistically significant at 90% confidence level.

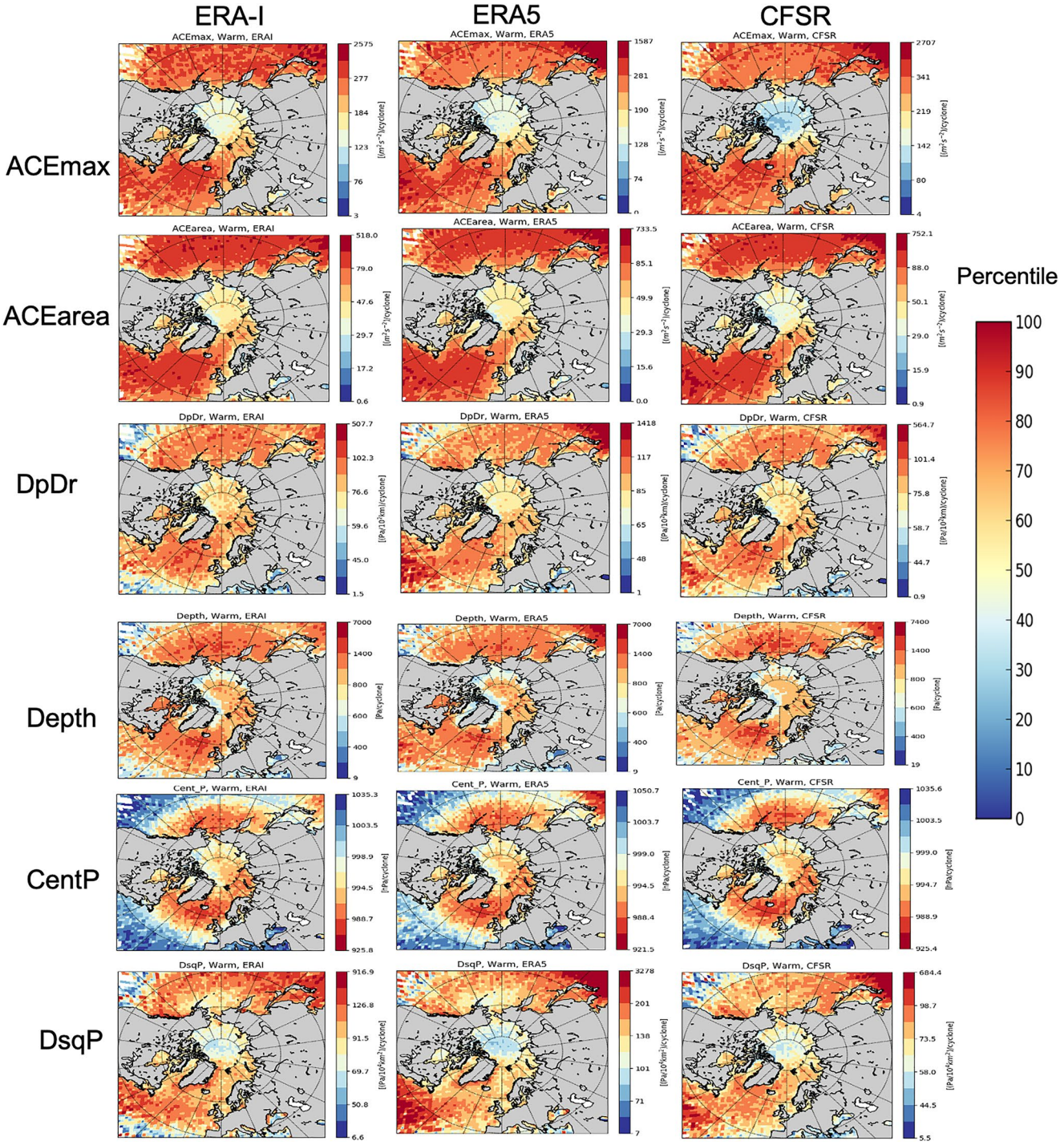

Figure A4. Different cyclone intensity metrics. The left column shows ERA-I data, middle column ERA5 data and right column CFSR. Results are for warm season. Intensity metrics were calculated as an average per cyclone in a 150 × 150 km grid box. The colormaps were normalized based on the percentile values, red colors depict strong cyclones, yellow colors average strength cyclones, and blue colors weaker cyclones.

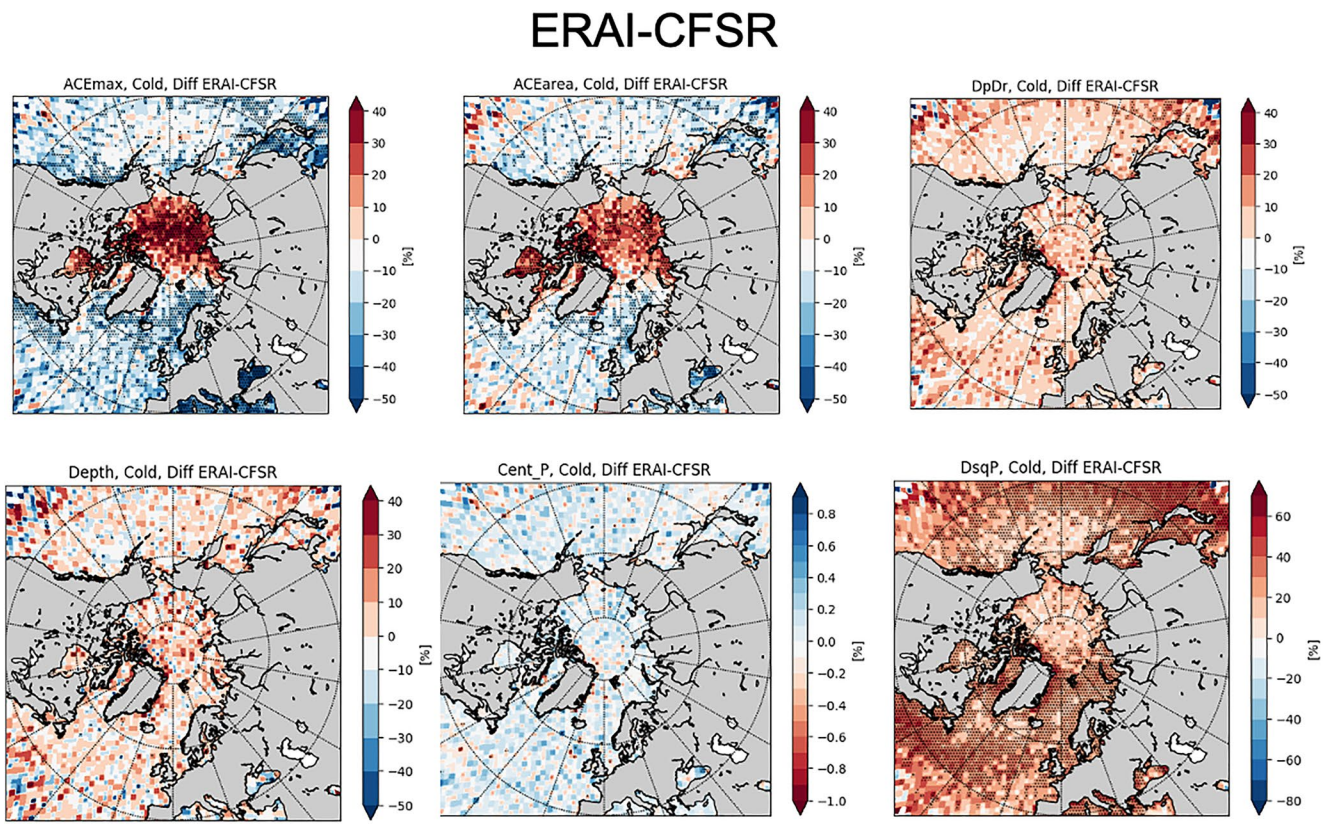

Figure A5. Differences in intensity metrics for the cold season (percentage change ERA-I minus CFSR compared to ERA-I). Red colors show positive change, blue colors negative change.

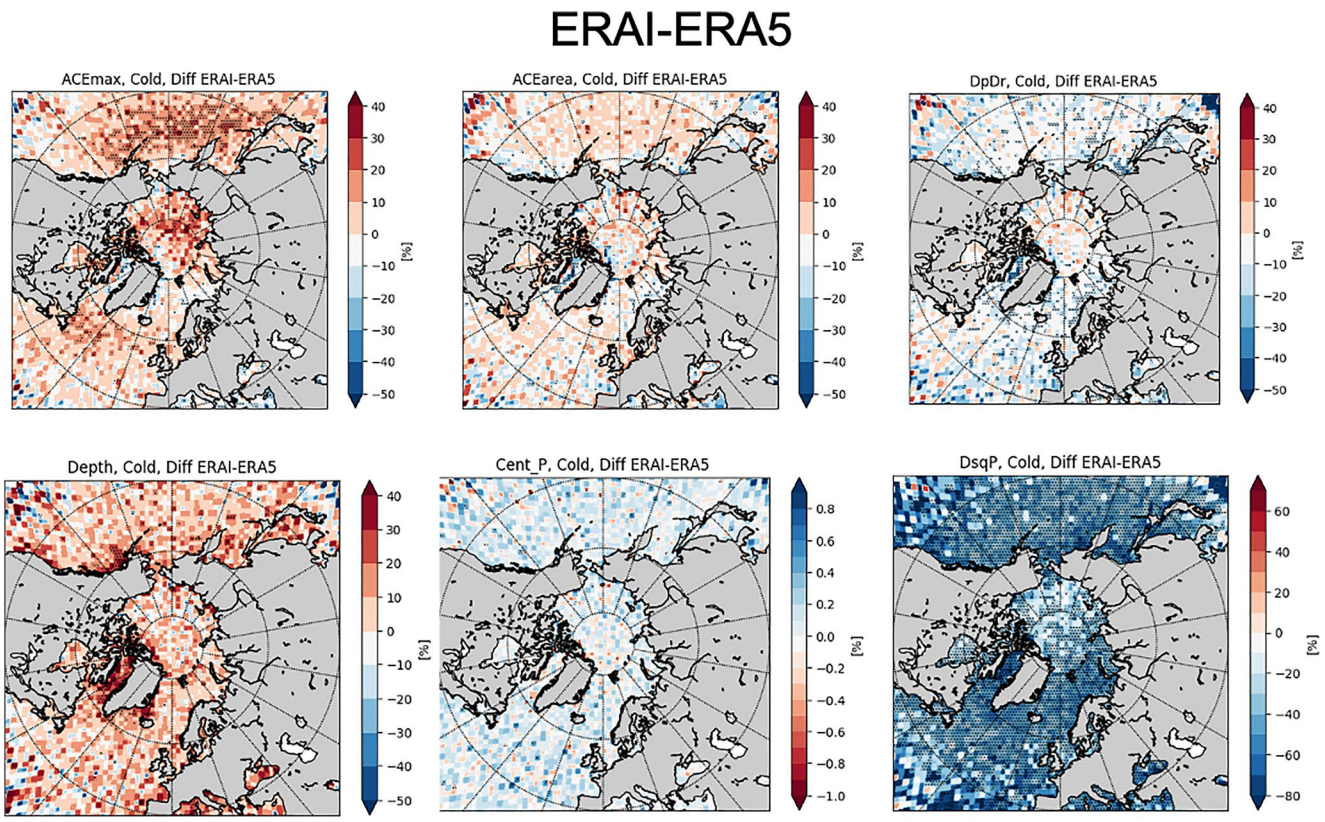

Figure A6. The differences in intensity metrics for the cold season (percentage change ERA-I minus ERA5 compared to ERAI). Red colors show positive change, blue colors negative change.

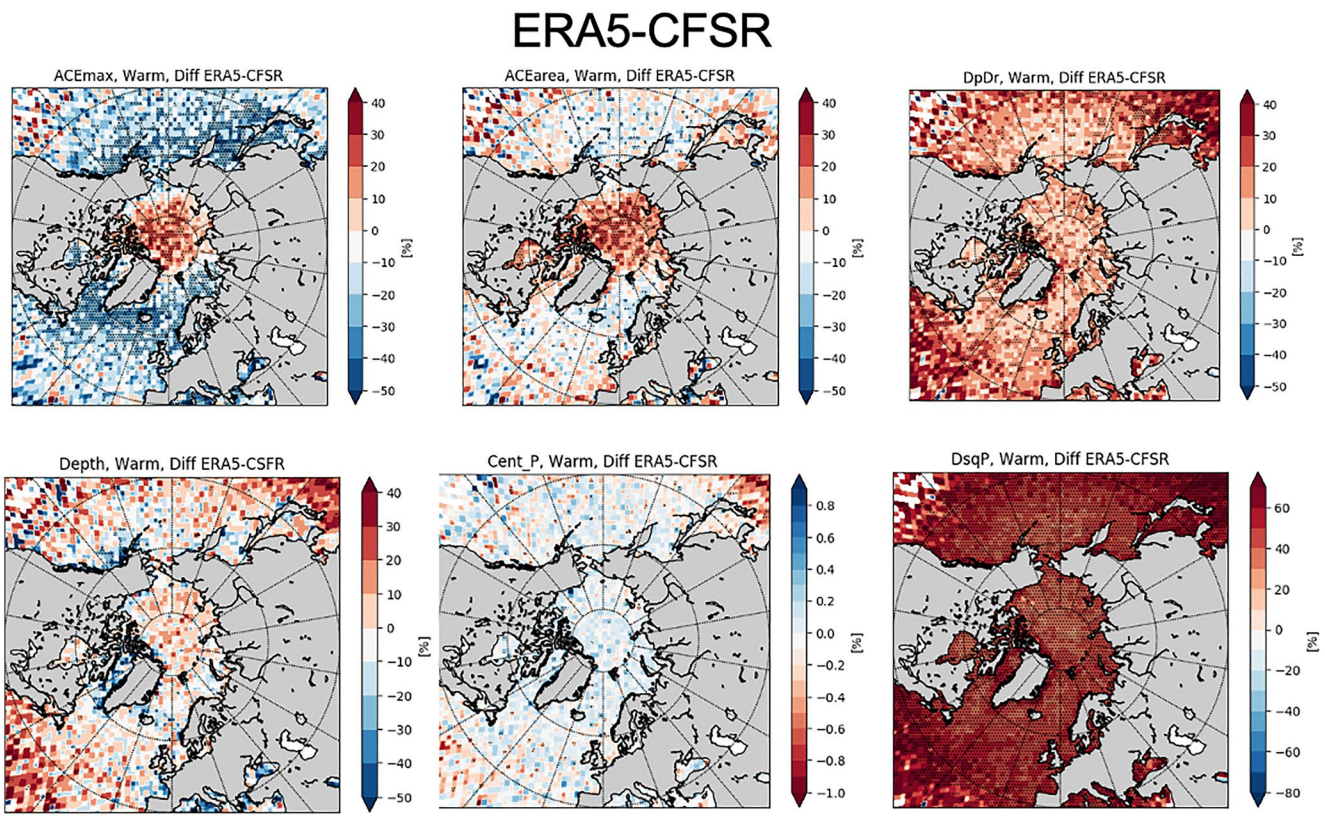

Figure A7. The differences in intensity metrics for the warm season (percentage change ERA5 minus CFSR compared to ERA5). Red colors show positive change, blue colors negative change.

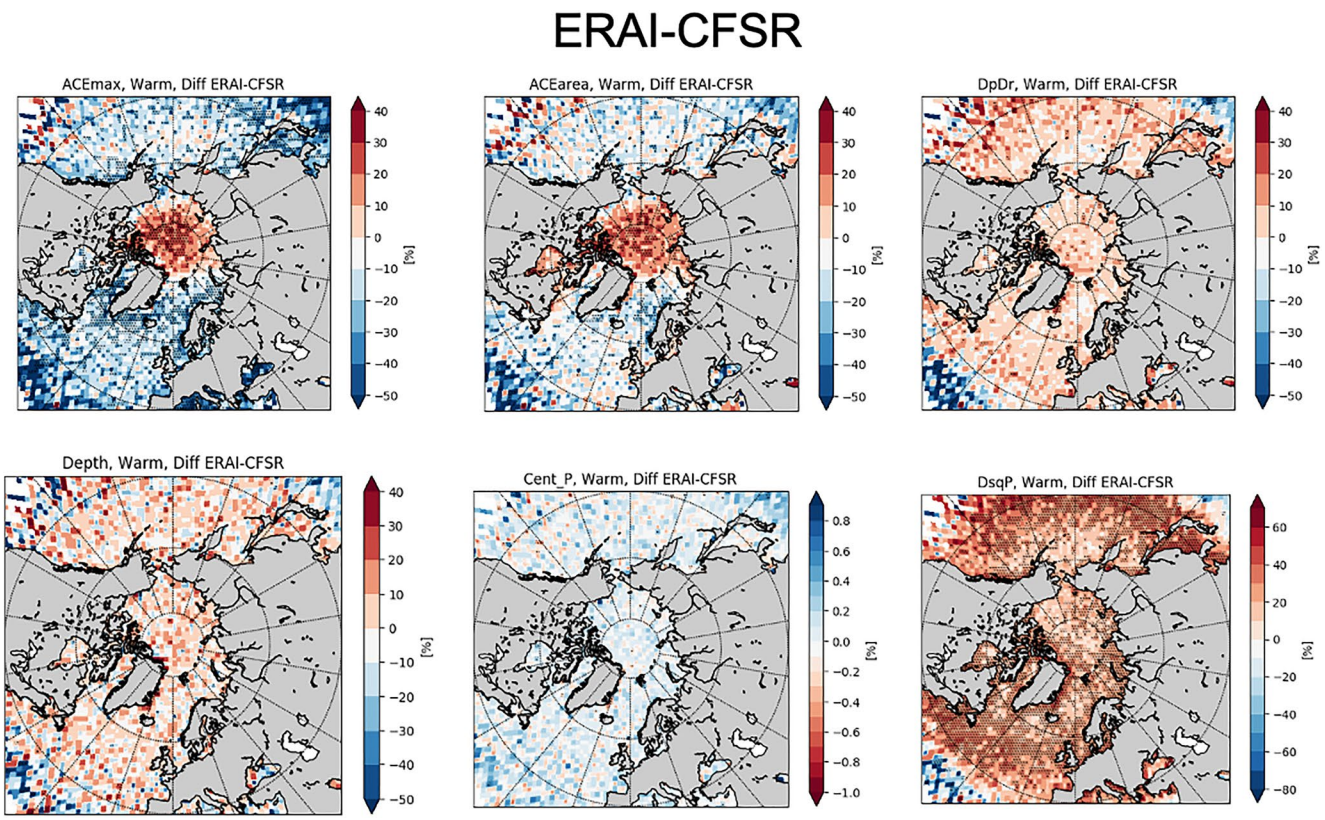

Figure A8. The differences in intensity metrics for the warm season (percentage change ERA-I minus CFSR compared to ERA-I). Red colors show positive change, blue colors negative change.

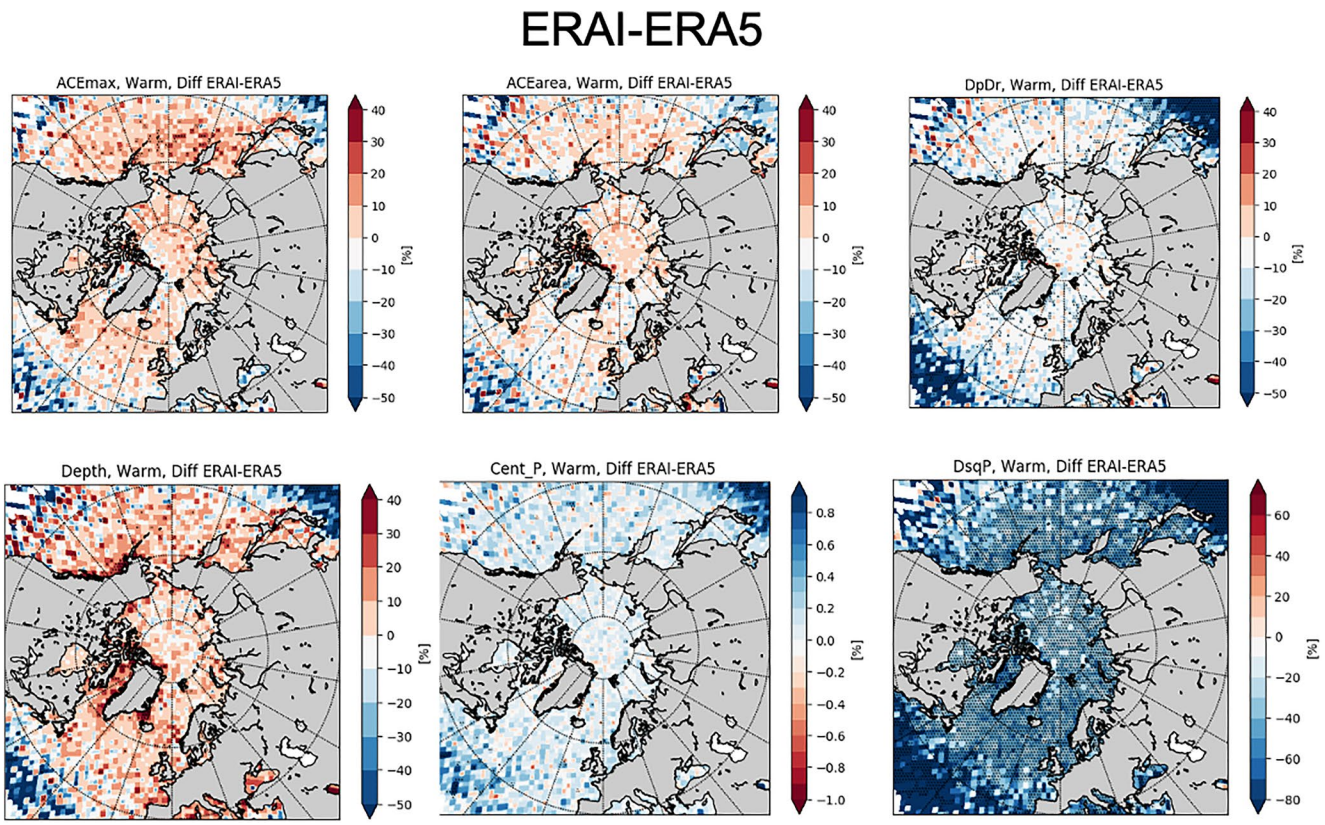

Figure A9. The differences in intensity metrics for the warm season (percentage change ERA-I minus ERA5 compared to ERAI). Red colors show positive change, blue colors negative change.

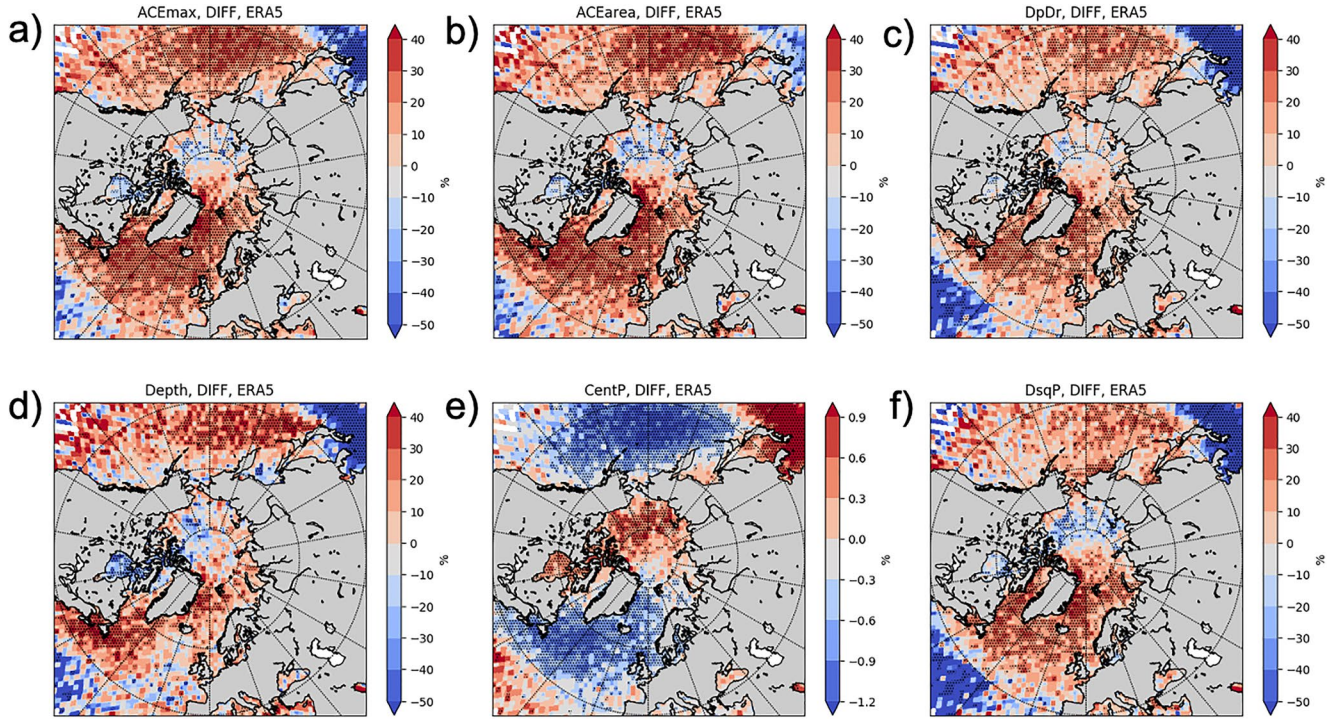

Figure A10. Difference in cyclone intensity between the seasons (cold minus warm) for ERA5 data. The difference is calculated as a percentage compared to cold season. Statistically significant areas, with 90% confidence level, are stippled. Red colors show positive difference, blue colors negative difference.

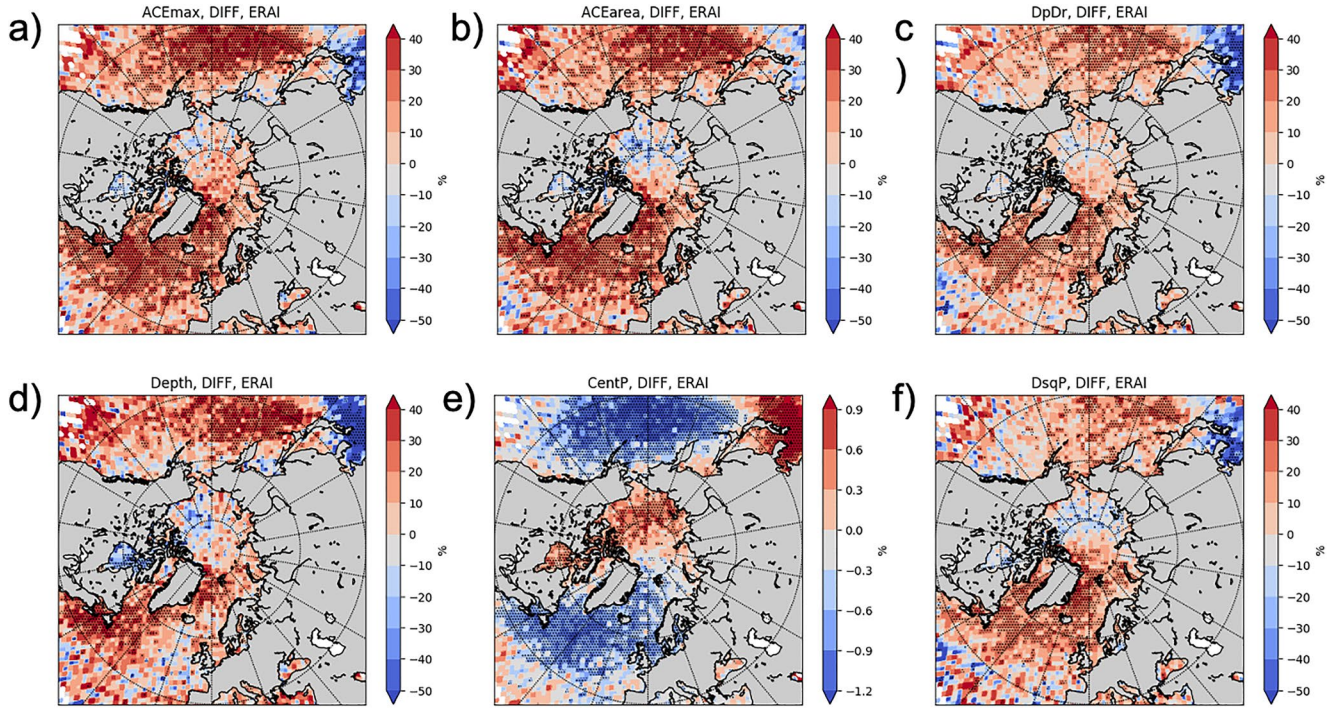

Figure A11. Difference in cyclone intensity between the seasons (cold minus warm) for ERA-I data. The difference is calculated as a percentage compared to cold season. Statistically significant areas, with 90% confidence level, are stippled. Red colors show positive difference, blue colors negative difference.

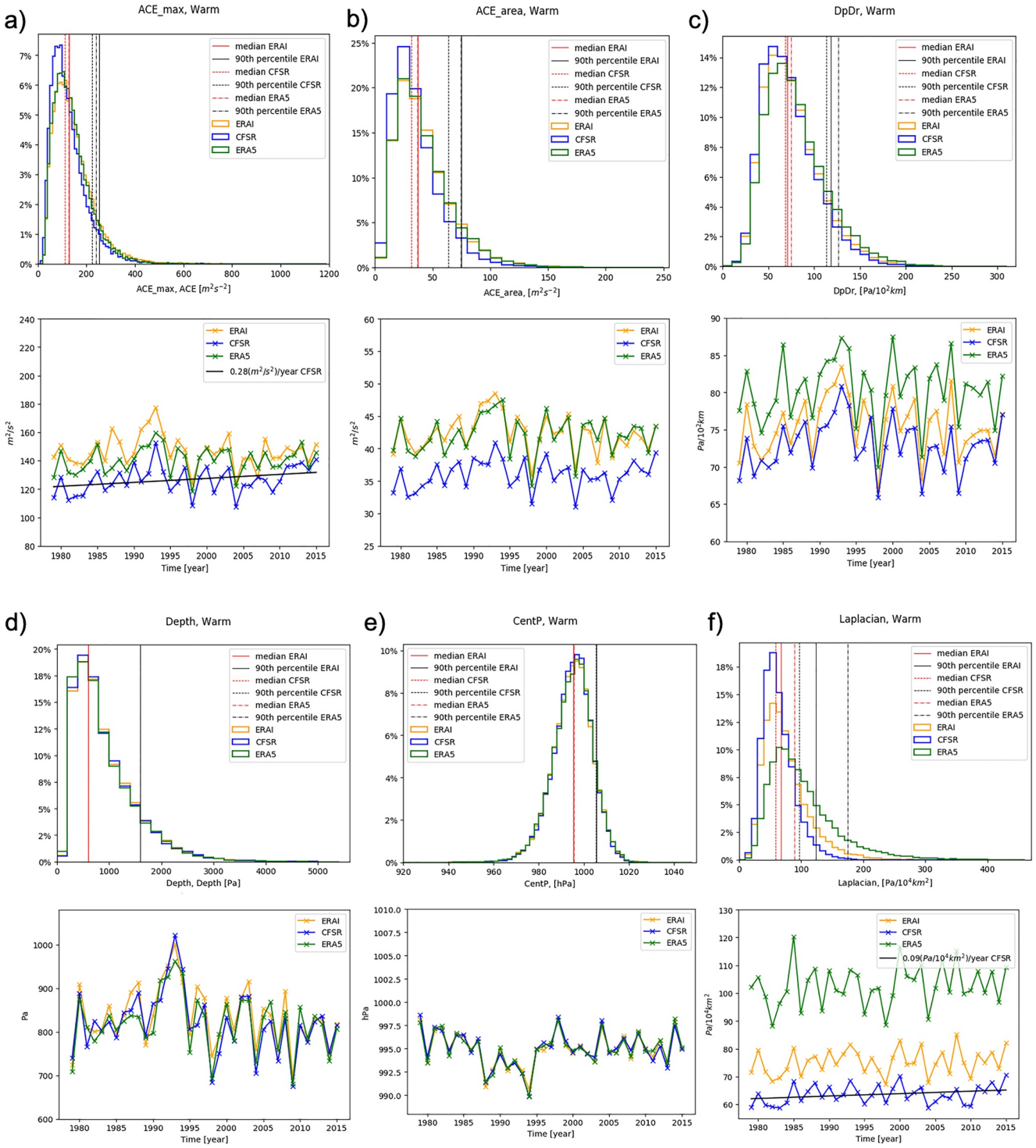

Figure A12. For each cyclone intensity metric during the warm season, the top figure shows histograms created using data from individual cyclone timesteps for ERA-I (yellow bars and solid lines), ERA5 (green bars and solid lines) and CFSR (blue bars and dashed lines). Vertical red (black) lines show median (90th percentile) values. The second row displays seasonal timeseries of the corresponding intensity metric using the same color scheme as the top row for each reanalysis dataset. Statistically significant trends at 90% confidence level are also shown (red lines for ERA-I green for ERA5 data, and black for CFSR).

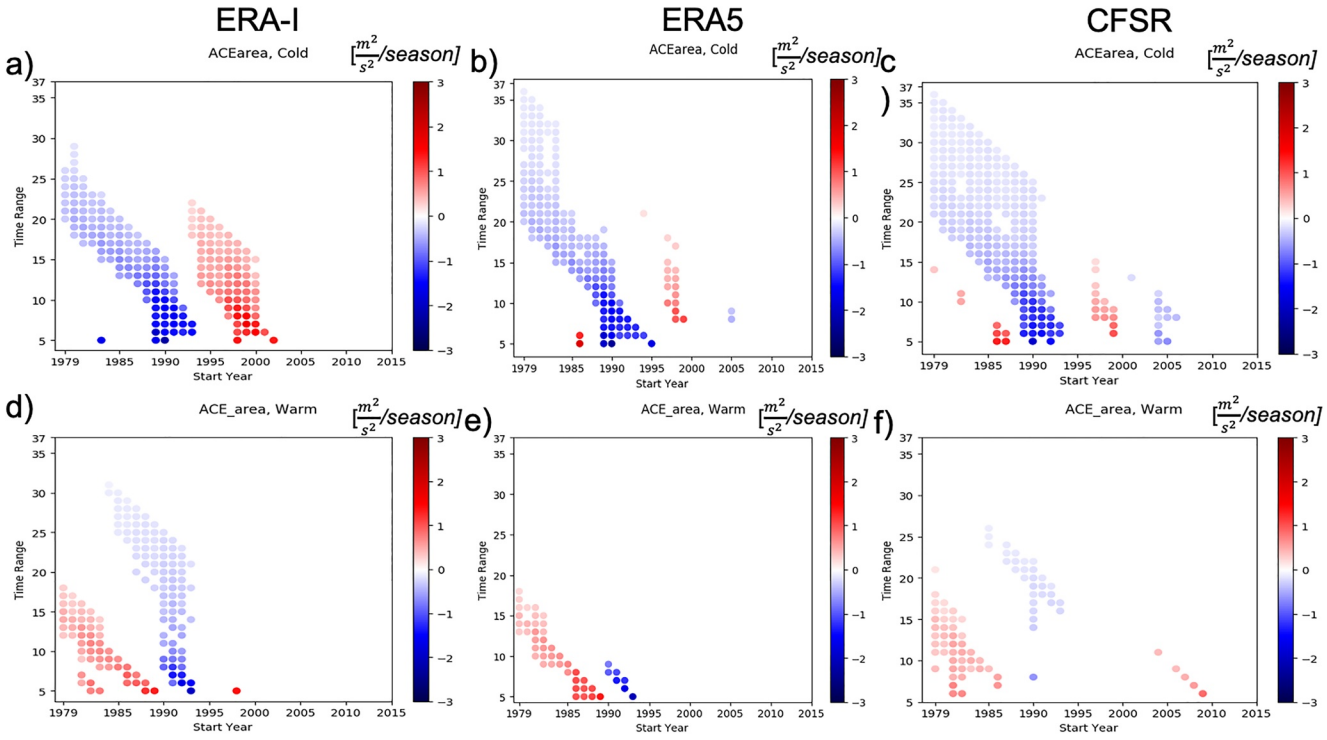

Figure A13. Trends for average ACEarea for different start years and time ranges. Red colors show positive trends, blue colors negative trends. All shown trends are statistically significant at 90% confidence level. Results are shown for cold (top row) and warm (bottom row) season for ERA-I (left column), ERA5 (middle column), and third for CFSR (right column). Units are $(\frac{m^2}{s^2})$/year.

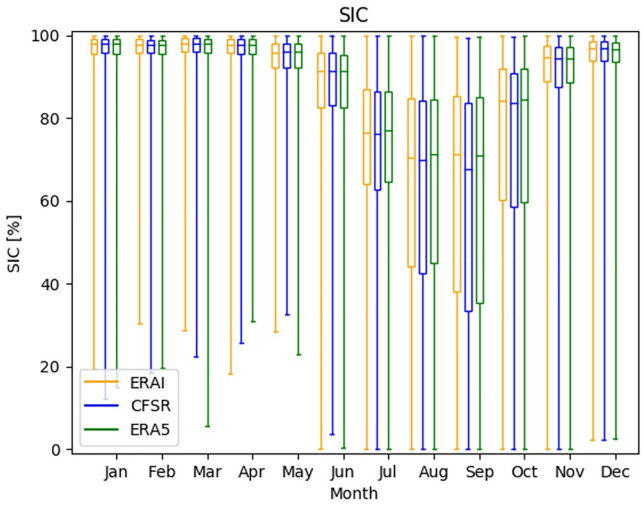

Figure A14. Monthly average cyclone area SIC experienced by the cyclones over the Arctic for each month for 1979–2015. The boxes show the interquartile range and median values and the whiskers the minimum and maximum values. Yellow colors show ERA-I data, green ERA5, and blue colors CFSR data.

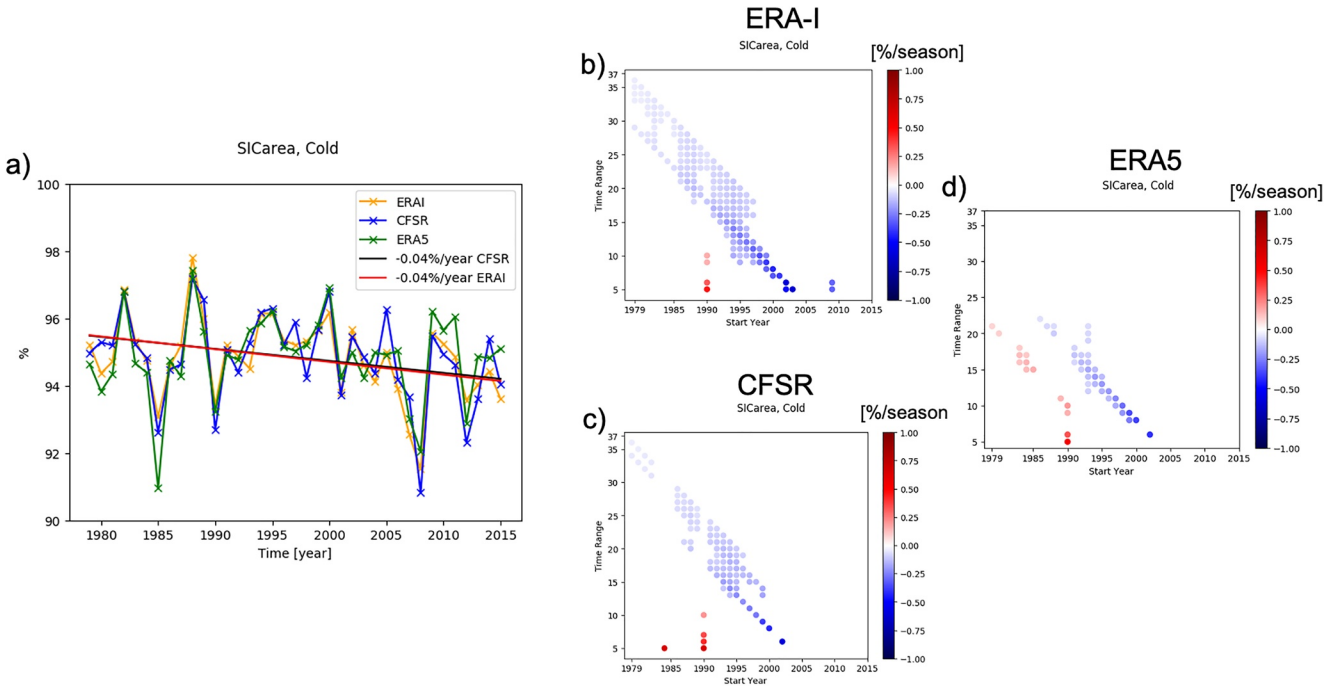

Figure A15. (a) Cold season timeseries of average SIC over the cyclone area for 1979–2015. Yellow color shows ERA-I data, green ERA5 and blue CFSR. The red line shows the significant trend for ERA-I data, green for ERA5 and black for CFSR. (b) Trends for average SIC for a cyclone for different start years and time ranges for ERA-I, (c) CFSR data and (d) ERA5 data. Blue colors show negative trends and red colors positive trends.

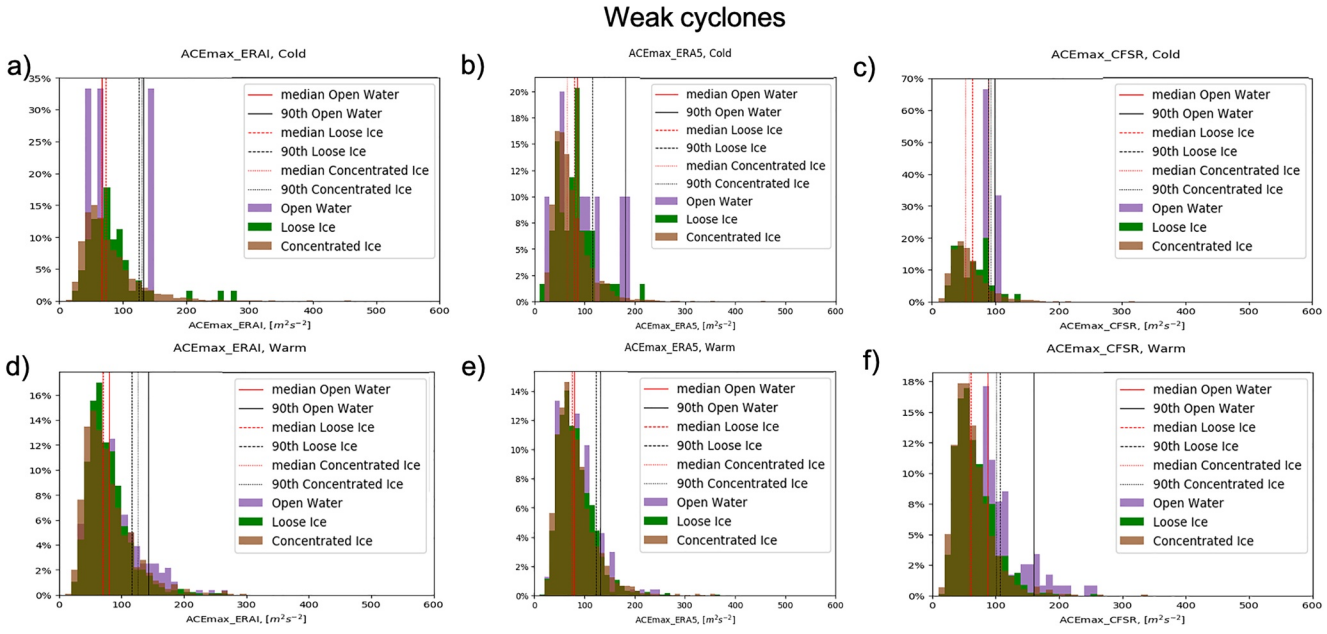

Figure A16. Histogram of ACEmax of weak cyclones for different surface states for the cold and warm seasons. Open water is shown in purple bars, loose sea ice in green bars, and concentrated ice in brown bars. Results from the cold season are in the top row and the warm season the bottom row. The median and 90th percentile values are shown by the red and black lines, respectively.

Data Availability Statement

Data sets for this research are available in these in-text data citation references: Cassano et al. (2021), Cavalieri et al. (1996), European Centre for Medium-Range Weather Forecasts (2012), Saha et al. (2010a), Saha et al. (2011), and European Centre for Medium-Range Weather Forecasts (2019).

Acknowledgments
We want to thank the three anonymous reviewers for their valuable comments that helped Cassano et al. (2021) improve the paper. This study was supported by National Science Foundation award PLR 1603384.

References

Alexander, M. A., Bhatt, U. S., Walsh, J. E., Timlin, M. S., Miller, J. S., & Scott, J. D. (2004). The atmospheric response to realistic Arctic sea ice anomalies in an AGCM during winter. *Journal of Climate*, *17*(5), 890–905. https://doi.org/10.1175/1520-0442(2004)017<0890:TARTRA>2.0.CO;2

Bader, J., Mesquita, M. D., Hodges, K. I., Keenlyside, N., Østerhus, S., & Miles, M. (2011). A review on Northern Hemisphere sea-ice, storminess and the North Atlantic oscillation: Observations and projected changes. *Atmospheric Research*, *101*(4), 809–834. https://doi.org/10.1016/j.atmosres.2011.04.007

Cassano, E., Valkonen, E., & Cassano, J. (2021). *Northern Hemisphere cyclone track data - Arctic Ocean focus 1979-2015*. Arctic Data Center. https://doi.org/10.18739/A2CZ3260W

Cavalieri, D. J., Parkinson, C. L., Gloersen, P., & Zwally, H. J. (1996). *Sea ice concentrations from Nimbus-7 SMMR and DMSP SSM/I-SSMIS Passive Microwave Data, Version 1*. NASA National Snow and Ice Data Center Distributed Active Archive Center. https://doi.org/10.5067/8GQ8LZQVL0VL

Crawford, A. D., & Serreze, M. C. (2016). Does the summer arctic frontal zone influence Arctic Ocean cyclone activity? *Journal of Climate*, *29*(13), 4977–4993. https://doi.org/10.1175/JCLI-D-15-0755.1

Dee, D. P., Uppala, S. M., Simmons, A. J., Berrisford, P., Poli, P., Kobayashi, S., et al. (2011). The ERA-Interim reanalysis: Configuration and performance of the data assimilation system. *Quarterly Journal of the Royal Meteorological Society*, *137*(656), 553–597. https://doi.org/10.1002/qj.828

ECMWF. (2006). *Chapter 10 - IFS documentation - Cy31r1 PART IV: Physical processes*. European Center fo Medium-Range Weather Forecasts.

ECMWF. (2016). *Chapter 3 - IFS Documentation - Cy41r2 PART IV: Physical processes*. European Center for Medium-Range Weather Forecasts.

European Centre for Medium-Range Weather Forecasts. (2012). *ERA-Interim Project, single parameter 6-hourly surface analysis and surface forecast time series*. Research Data Archive at the National Center for Atmospheric Research, Computational and Information Systems Laboratory. https://doi.org/10.5065/D64747WN

European Centre for Medium-Range Weather Forecasts. (2019). *ERA5 Reanalysis (0.25 degree latitude-longitude grid)*. Research Data Archive at the National Center for Atmospheric Research, Computational and Information Systems Laboratory. https://doi.org/10.5065/BH6N-5N20

Francis, J. A., Chan, W., Leathers, D. J., Miller, J. R., & Veron, D. E. (2009). Winter Northern Hemisphere weather patterns remember summer Arctic sea-ice extent. *Geophysical Research Letters*, *36*. https://doi.org/10.1029/2009GL037274

Graham, R. M., Itkin, P., Meyer, A., Sundfjord, A., Spreen, G., Smedsrud, L. H., et al. (2019). Winter storms accelerate the demise of sea ice in the Atlantic sector of the Arctic Ocean. *Scientific Reports*, *9*(1), 9222. https://doi.org/10.1038/s41598-019-45574-5

Hersbach, H., Bell, B., Berrisford, P., Hirahara, S., Horányi, A., Muñoz-Sabater, J., et al. (2020). The ERA5 global reanalysis. *Quarterly Journal of the Royal Meteorological Society*, *146*(730), 1999–2049. https://doi.org/10.1002/qj.3803

Jaiser, R., Dethloff, K., Handorf, D., Rinke, A., & Cohen, J. (2012). Impact of sea ice cover changes on the Northern Hemisphere atmospheric winter circulation. *Tellus A: Dynamic Meteorology and Oceanography*, *64*(1), 11595. https://doi.org/10.3402/tellusa.v64i0.11595

Jakobson, E., Vihma, T., Palo, T., Jakobson, L., Keernik, H., & Jaagus, J. (2012). Validation of atmospheric reanalyzes over the central Arctic Ocean. *Geophysical Research Letters*, *39*. https://doi.org/10.1029/2012GL051591

Jakobson, L., Vihma, T., & Jakobson, E. (2019). Relationships between sea ice concentration and wind speed over the Arctic Ocean during 1979–2015. *Journal of Climate*, *32*(22), 7783–7796. https://doi.org/10.1175/jcli-d-19-0271.1

Klotzbach, P. J. (2006). Trends in global tropical cyclone activity over the past twenty years (1986–2005). *Geophysical Research Letters*, *33*. https://doi.org/10.1029/2006GL025881

Koyama, T., Stroeve, J., Cassano, J., & Crawford, A. (2017). Sea ice loss and arctic cyclone activity from 1979 to 2014. *Journal of Climate*, *30*(12), 4735–4754. https://doi.org/10.1175/JCLI-D-16-0542.1

Lindsay, R., Wensnahan, M., Schweiger, A., & Zhang, J. (2014). Evaluation of seven different atmospheric reanalysis products in the Arctic*. *Journal of Climate*, *27*(7), 2588–2606. https://doi.org/10.1175/JCLI-D-13-00014.1

Martin, T., Steele, M., & Zhang, J. (2014). Seasonality and long-term trend of Arctic Ocean surface stress in a model. *Journal of Geophysical Research: Oceans*, *119*, 1723–1738. https://doi.org/10.1002/2013JC009425

Maslanik, J. A., Fowler, C., Stroeve, J., Drobot, S., Zwally, J., Yi, D., & Emery, W. (2007). A younger, thinner Arctic ice cover: Increased potential for rapid, extensive sea-ice loss. *Geophysical Research Letters*, *34*. https://doi.org/10.1029/2007GL032043

McCabe, G. J., Clark, M. P., & Serreze, M. C. (2001). Trends in Northern Hemisphere surface cyclone frequency and intensity. *Journal of Climate*, *14*(12), 2763–2768. https://doi.org/10.1175/1520-0442(2001)014<2763:TINHSC>2.0.CO;2

Murray, R. J., & Simmonds, I. (1991). A numerical scheme for tracking cyclone centres from digital data Part I: Development and operation of the scheme. *Australian Meteorological Magazine*, *39*, 155–166.

Onarheim, I. H., Eldevik, T., Smedsrud, L. H., & Stroeve, J. C. (2018). Seasonal and regional manifestation of Arctic sea ice loss. *Journal of Climate*, *31*(12), 4917–4932. https://doi.org/10.1175/JCLI-D-17-0427.1

Overland, J. E., & Wang, M. (2010). Large-scale atmospheric circulation changes are associated with the recent loss of Arctic sea ice. *Tellus A: Dynamic Meteorology and Oceanography*, *62*(1), 1–9. https://doi.org/10.1111/j.1600-0870.2009.00421.x

Parkinson, C. L., & Comiso, J. C. (2013). On the 2012 record low Arctic sea ice cover: Combined impact of preconditioning and an August storm. *Geophysical Research Letters*, *40*, 1356–1361. https://doi.org/10.1002/grl.50349

Rinke, A., Maslowski, W., Dethloff, K., & Clement, J. (2006). Influence of sea ice on the atmosphere: A study with an Arctic atmospheric regional climate model. *Journal of Geophysical Research*, *111*. https://doi.org/10.1029/2005JD006957

Rudeva, I., & Simmonds, I. (2015). Variability and trends of global atmospheric frontal activity and links with large-scale modes of variability. *Journal of Climate*, *28*(8), 3311–3330. https://doi.org/10.1175/JCLI-D-14-00458.1

Saha, S., Moorthi, S., Pan, H.-L., Wu, X., Wang, J., Nadiga, S., et al. (2010a). *NCEP Climate Forecast System Reanalysis (CFSR) 6-hourly products, January 1979 to December 2010*. Research Data Archive at the National Center for Atmospheric Research, Computational and Information Systems Laboratory. https://doi.org/10.5065/D69K487J

Saha, S., Moorthi, S., Pan, H.-L., Wu, X., Wang, J., Nadiga, S., et al. (2010b). The NCEP climate forecast system reanalysis. *Bulletin of the American Meteorological Society*, *91*(8), 1015–1058. https://doi.org/10.1175/2010BAMS3001.1

Saha, S., Moorthi, S., Wu, X., Wang, J., Nadiga, S., Tripp, P., et al. (2011). *NCEP Climate Forecast System Version 2 (CFSV2) 6-hourly products*. Research Data Archive at the National Center for Atmospheric Research, Computational and Information Systems Laboratory. https://doi.org/10.5065/D61C1TXF

Saha, S., Moorthi, S., Wu, X., Wang, J., Nadiga, S., Tripp, P., et al. (2014). The NCEP climate forecast system version 2. *Journal of Climate*, *27*(6), 2185–2208. https://doi.org/10.1175/JCLI-D-12-00823.1

Schweiger, A. J., Lindsay, R. W., Vavrus, S., & Francis, J. A. (2008). Relationships between Arctic sea ice and clouds during autumn. *Journal of Climate*, *21*(18), 4799–4810. https://doi.org/10.1175/2008JCLI2156.1

Screen, J. A., & Simmonds, I. (2010). The central role of diminishing sea ice in recent Arctic temperature amplification. *Nature*, *464*(7293), 1334–1337. https://doi.org/10.1038/nature09051

Screen, J. A., Simmonds, I., Deser, C., & Tomas, R. (2013). The atmospheric response to three decades of observed Arctic sea ice loss. *Journal of Climate*, *26*(4), 1230–1248. https://doi.org/10.1175/JCLI-D-12-00063.1

Sepp, M., & Jaagus, J. (2011). Changes in the activity and tracks of Arctic cyclones. *Climatic Change*, *105*(3), 577–595. https://doi.org/10.1007/s10584-010-9893-7

Serreze, M. C. (1995). Climatological aspects of cyclone development and decay in the Arctic. *Atmosphere-Ocean*, *33*(1), 1–23. https://doi.org/10.1080/07055900.1995.9649522

Serreze, M. C., & Barrett, A. P. (2008). The summer cyclone maximum over the Central Arctic Ocean. *Journal of Climate*, *21*(5), 1048–1065. https://doi.org/10.1175/2007JCLI1810.1

Serreze, M. C., Barrett, A. P., Stroeve, J. C., Kindig, D. N., & Holland, M. M. (2009). The emergence of surface-based Arctic amplification. *The Cryosphere*, *3*(1), 11–19. https://doi.org/10.5194/tc-3-11-2009

Serreze, M. C., Lynch, A. H., & Clark, M. P. (2001). The Arctic frontal zone as seen in the NCEP–NCAR reanalysis. *Journal of Climate*, *14*(7), 1550–1567. https://doi.org/10.1175/1520-0442(2001)014<1550:TAFZAS>2.0.CO;2

Simmonds, I., Burke, C., & Keay, K. (2008). Arctic climate change as manifest in cyclone behavior. *Journal of Climate*, *21*(22), 5777–5796. https://doi.org/10.1175/2008JCLI2366.1

Simmonds, I., & Keay, K. (2009). Extraordinary September Arctic sea ice reductions and their relationships with storm behavior over 1979–2008. *Geophysical Research Letters*, *36*. https://doi.org/10.1029/2009GL039810

Stroeve, J., Serreze, M., Drobot, S., Gearheard, S., Holland, M., Maslanik, J., et al., (2008). Arctic sea ice extent plummets in 2007. *EOS, Transactions American Geophysical Union*, *89*. https://doi.org/10.1029/2008EO020001

Stroeve, J. C., Kattsov, V., Barrett, A., Serreze, M., Pavlova, T., Holland, M., & Meier, W. N. (2012). Trends in Arctic sea ice extent from CMIP5, CMIP3 and observations. *Geophysical Research Letters*, *39*. https://doi.org/10.1029/2012GL052676

Tastula, E.-M., Vihma, T., Andreas, E. L., & Galperin, B. (2013). Validation of the diurnal cycles in atmospheric reanalyzes over Antarctic sea ice. *Journal of Geophysical Research: Atmospheres*, *118*, 4194–4204. https://doi.org/10.1002/jgrd.50336

Ulbrich, U., Leckebusch, G. C., & Pinto, J. G. (2009). Extra-tropical cyclones in the present and future climate: A review. *Theoretical and Applied Climatology*, *96*(1), 117–131. https://doi.org/10.1007/s00704-008-0083-8

Varino, F., Arbogast, P., Joly, B., Riviere, G., Fandeur, M.-L., Bovy, H., & Granier, J.-B. (2018). Northern Hemisphere extratropical winter cyclones variability over the 20th century derived from ERA-20C reanalysis. *Climate Dynamics*, *52*(1), 1027–1048. https://doi.org/10.1007/s00382-018-4176-5

Vessey, A. F., Hodges, K. I., Shaffrey, L. C., & Day, J. J. (2020). An inter-comparison of Arctic synoptic scale storms between four global reanalysis datasets. *Climate Dynamics*, *54*(5), 2777–2795. https://doi.org/10.1007/s00382-020-05142-4

Vihma, T. (2014). Effects of Arctic sea ice decline on weather and climate: A review. *Surveys in Geophysics*, *35*(5), 1175–1214. https://doi.org/10.1007/s10712-014-9284-0

Wernli, H., & Schwierz, C. (2006). Surface cyclones in the ERA-40 Dataset (1958–2001). Part I: Novel identification method and global climatology. *Journal of the Atmospheric Sciences*, *63*(10), 2486–2507. https://doi.org/10.1175/JAS3766.1

Wickström, S., Jonassen, M. O., Vihma, T., & Uotila, P. (2019). Trends in cyclones in the high-latitude North Atlantic during 1979–2016. *Quarterly Journal of the Royal Meteorological Society*, *146*(727), 762–779. https://doi.org/10.1002/qj.3707

Yamamoto, K., Tachibana, Y., Honda, M., & Ukita, J. (2006). Intra-seasonal relationship between the Northern Hemisphere sea ice variability and the North Atlantic oscillation. *Geophysical Research Letters*, *33*. https://doi.org/10.1029/2006GL026286

Zahn, M., Akperov, M., Rinke, A., Feser, F., & Mokhov, I. I. (2018). Trends of cyclone characteristics in the Arctic and their patterns from different reanalysis data. *Journal of Geophysical Research: Atmospheres*, *123*, 2737–2751. https://doi.org/10.1002/2017JD027439

Zhang, J., Lindsay, R., Schweiger, A., & Steele, M. (2013). The impact of an intense summer cyclone on 2012 Arctic sea ice retreat. *Geophysical Research Letters*, *40*, 720–726. https://doi.org/10.1002/grl.50190

Zhang, X., Walsh, J. E., Zhang, J., Bhatt, U. S., & Ikeda, M. (2004). Climatology and interannual variability of Arctic cyclone activity: 1948–2002. *Journal of Climate*, *17*(12), 2300–2317. https://doi.org/10.1175/1520-0442(2004)017<2300:CAIVOA>2.0.CO;2